AD-A107 029 UNITED TECHNOLOGIES RESEARCH CENTER EAST HARTFORD CT F/G 21/2
INVESTIGATION OF COMBUSTION PROCESS USING FIBER OPTICS.(U)
JUN 81 W W MOREY N00019-80-C-0331
UNCLASSIFIED UTRC/R81-925172-4 NL

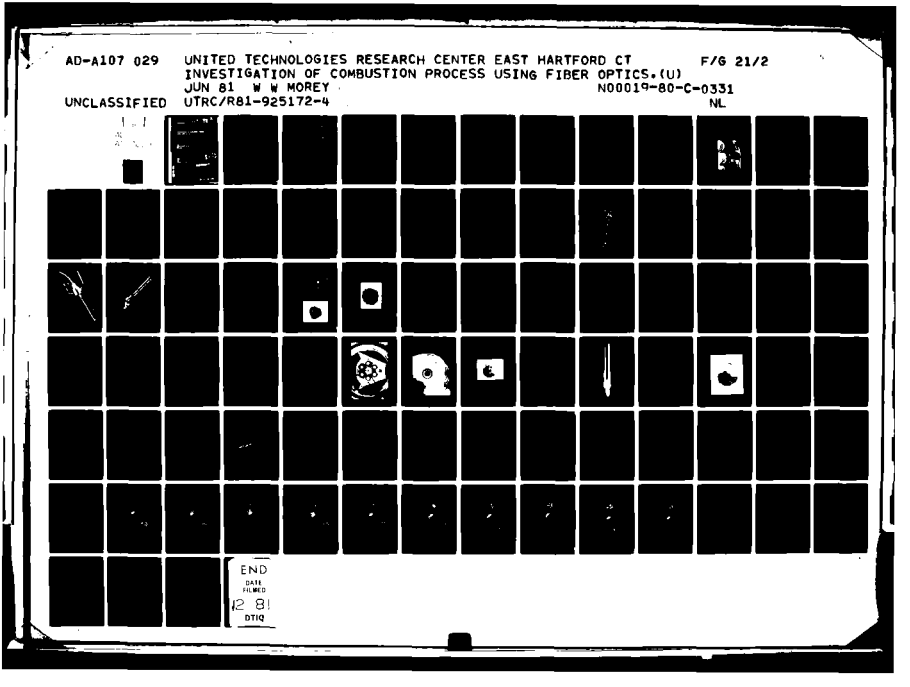

END
DATE FILMED
12 81
DTIC

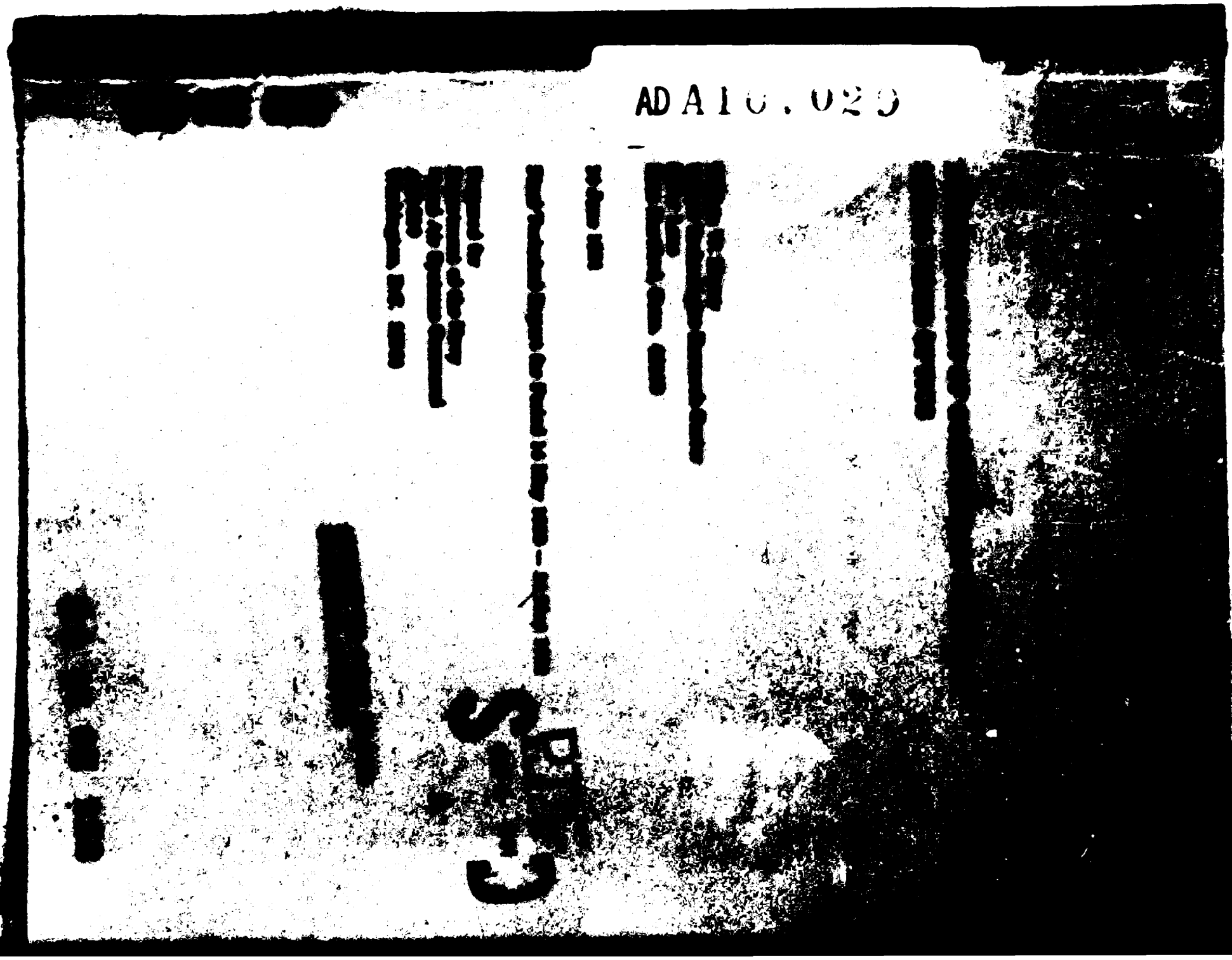
AD A1C . 029

Report R81-925172-4

INVESTIGATION OF COMBUSTION PROCESS USING FIBER OPTICS

William W. Morey
United Technologies Research Center
Silver Lane
East Hartford, Conn. 06108

14 June 1981

Final Technical Report for Period 14 May 1980 - 14 May 1981

Prepared for
Department of the Navy
Naval Air Systems Command
AIR-310
Washington, D.C. 20361

SECURITY CLASSIFICATION OF THIS PAGE (When Data Entered)

REPORT DOCUMENTATION PAGE	READ INSTRUCTIONS BEFORE COMPLETING FORM
1 REPORT NUMBER	2 GOVT ACCESSION NO. AD A107021 / 3 RECIPIENT'S CATALOG NUMBER
4 TITLE (and Subtitle) Investigation of Combustion Process Using Fiber Optics	5 TYPE OF REPORT & PERIOD COVERED Final Technical Report 6 PERFORMING ORG. REPORT NUMBER R81-925172-4
7 AUTHOR(s) William W. Morey	8 CONTRACT OR GRANT NUMBER(s) N00019-80-C-0331
9 PERFORMING ORGANIZATION NAME AND ADDRESS United Technologies Research Center Silver Lane East Hartford, Conn. 06108	10 PROGRAM ELEMENT, PROJECT, TASK AREA & WORK UNIT NUMBERS
11 CONTROLLING OFFICE NAME AND ADDRESS Naval Air Systems Command AIR-30 Washington, D.C. 20361	12 REPORT DATE 14 Jun 81 13 NUMBER OF PAGES 81
14 MONITORING AGENCY NAME & ADDRESS(if different from Controlling Office)	15 SECURITY CLASS. (of this report) 15a. DECLASSIFICATION DOWNGRADING SCHEDULE

16. DISTRIBUTION STATEMENT (of this Report)

APPROVED FOR PUBLIC RELEASE; DISTRIBUTION UNLIMITED

17. DISTRIBUTION STATEMENT (of the abstract entered in Block 20, if different from Report)

18. SUPPLEMENTARY NOTES

19. KEY WORDS (Continue on reverse side if necessary and identify by block number)

Combustion, Fiber Optics, Fiberscope

20. ABSTRACT (Continue on reverse side if necessary and identify by block number)

This technical report describes the results of a 12 month program to design, build, and test a fiber optic viewing device (fiberscope) on a high pressure gas turbine combustor rig. High speed motion picture photography along with video tapings were made of the combustor flame with the fiberscope. With the high speed photography the turbulent flame motion could be followed in some detail. Visible wavelength spectra were

DD FORM 1 JAN 73 1473 EDITION OF 1 NOV 65 IS OBSOLETE S/N 0102-LF-014-6601

SECURITY CLASSIFICATION OF THIS PAGE (When Data Entered)

taken of the flame emission through the fiberscope and analysis indicates that a mean flame temperature can be measured. The fluctuation frequency spectrum of the flame was also observed with a fast fourier transform analyzer, and the possibility of coupling with acoustic resonances was indicated. In addition, the fuel spray was illuminated with laser light from the fiberscope probe and contour plots were made of a sequence of frames from the movie film.

The combustor viewing probe may be used as an important aid in future combustion design and to help determine causes of various failure modes of combustor liners.

FOREWORD

This technical report summarizes the results of a twelve month program to investigate the use of optical fibers for viewing the combustion process in an operating gas turbine combustor. The program was supported by the Department of the Navy, Naval Air Systems Command under contract number N00019-80-C-0331. The report was prepared by the Applied Physics Laboratory at the United Technologies Research Center (UTRC), East Hartford, Connecticut. Dr. William W. Morey was the Principal Investigator for the program. Engineering design assistance was provide by R. F. Dondero. Helpful engineering advise and operation of the combustor was provided by J. B. Kennedy. Technical Assistance for the program was provided by A. L. Wilson, D. N. Dastous, D. Terza, R. E. LaBarre and several others who helped make the program sucessful. Helpful discussions on several technical aspects of the program were given by W. H. Glenn, J. R. Dunphy, and E. Snitzer.

The inclusive dates of research on this program were 14 May 1980 to 14 May 1981. The final report was submitted by the author in July 1981.

TABLE OF CONTENTS

TABLE OF CONTENTS (Cont'd)

LIST OF FIGURES

1. INTRODUCTION AND SUMMARY

1.1 Background. For several years now, optical viewing systems have been used in aircraft engine and engine test rigs. Viewing systems have been developed for monitoring blade tip clearances, knife edge seal positions, and turbine vane clearances and for inspection of blade and vane damage on engines when they are not in operation (Refs. 1, 2). Also, optical pyrometers have been developed and used to measure turbine blade temperatures (Ref. 3). The idea of using coherent fiber optic viewing devices, or fiberscopes, to view the inside of operating gas turbine combustors was suggested over two years ago in response to several existing problems with the durability of combustor liners and turbine vanes. With new advances in engine design requiring efficient combustion and operation at higher temperatures, combustor design and durability become even more critical. All aspects of combustor design are not fully understood; and the viewing probe can prove useful in helping to understand their operation and failure modes.

Both the hostile environment and limited access of a gas turbine combustor make it difficult to determine and analyze characteristics of combustion "in situ", during full scale engine operation. Being able to visualize and measure the characteristics of flame dynamics including location and motion of the flame and the occurrence of hot streaks at the turbine inlet along with flame color temperature measurements would be an important aid for future advanced combustor designs. Observations on flame motion and turbulence may be related to the efficiency of mixing fuel and air. An improper mixing, for instance, could lead to a fuel rich region that creates an extended burning zone traveling down the combustor and into the turbine inlet. Such occurrences cause overheating and damage to the turbine vanes. A viewing probe can also observe if and under what engine operating conditions the luminous flame impinges either continuously or intermittently on the liner wall. Such a flame pattern creates localized high metal temperatures that lead to liner crack formation, buckling, and burn-through. Figure 1.1 shows an example of a damaged liner wall. The flame was probably striking the surface at the damaged sites. Ignition and burning in recirculation zones that may affect flame dynamics can also be observed with the fiberscope. It may also be possible that a component of the flame motion could be coupled to acoustic resonances in the combustor as discussed by Gaydon (Ref. 4, Ch. 7). The occurrence of such resonances may misdirect flame patterns and couple acoustically to other engine components.

Besides flame dynamics and temperature, another important use of a viewing probe would be to observe and inspect the inside or outside surface of the combustor liner for overheating, fatigue cracking, and formation of hard carbon deposits. The probe could tell when and under what conditions these problems occur and follow the course of their development, during engine operation. The surface inspection would require proper illumination

FIG. 1.1

BURNER LINER FAILURE MODES

81-2-150-3

either from an external source or from the flame luminosity. Examination of other components in the combustor such as fuel nozzles, flame holders, and spray patterns may also be achieved with proper probe placement, articulation, and illumination. An external illumination source could be provided with a laser and a single fiber or with an arc lamp and a bundle of fibers used in conjunction with the viewing probe.

1.2 Program Objectives. The objective of this program was to design, construct, and integrate a fiber optic viewing probe (or fiberscope) onto a high pressure gas turbine combustor rig. Visual images of the flame from inside the combustor were to be taken and several diagnostic and image analysis techniques were to be examined that used the combustor image from the fiberscope. A laser illuminating fiber was also included in the probe. The results of the program are to be used for the future design and employment of a viewing system on an operating gas turbine engine, and to learn what types of practical diagnostic measurements can be made from a viewing probe and illuminator system.

1.3 Program Summary. The viewing probe was run successfully with the accumulation of several hours of operation on a high pressure combustor rig. The probe and illuminator were placed on the combustor to view downstream into the combustion zone from a position between fuel nozzles. This was the coolest place to put the viewing probe since it is primarily exposed to the combustor inlet temperatures. Thermocouple measurements indicated that the probe was more than adequately cooled with a steady flow of nitrogen gas. Part of the nitrogen flow was directed onto the viewing lens surface at the probe tip to keep it free of sooting deposites which are quite dense on that part of the combustor liner where the probe tip was exposed.

Before operation on the combustor, the fiberscope was tested for durability and optical alignment on a small test cell. In the test cell the fiberscope was subjected to temperatures and pressures expected in the combustor rig and vibrated over a wide range of frequencies. The optical system was also characterized for resolution, field-of-view, wavelength transmission and angular response.

Several different recordings and measurements were made from the combustor view including 35 mm photographs, high speed motion pictures, video tape, wavelength spectra, flame turbulence spectra, and laser illumination. Using a wide range of exposures, 35 mm color photographs were taken of the combustor view along with red, green, and blue filters. The fastest shutter speeds of 1/2000 sec gave adequate exposures with the 400 ASA film pushed one stop in development. The slower shutter speeds gave a time averaging to the flame and removed the flame structure that was visible in the fast exposures.

1100 feet of color motion pictures were also taken from the combustor view. Framing rates from 100 to 5000 frames/sec were used with Locam and Hycam cameras. The flame motion was reduced in speed by over 200 times at the 5000 frame/sec rate. A series of 12 frames from the movie was digitized and contour plots made. In the progression of frames, the flame from the upper nozzle can be seen to break in two pieces and move out of the combustor.

The framing rate of a video camera is only 33 frames per second with two interlacing scans during each frame. As a consequence, the video pictures could not follow flame motion or see flame structure as was done with the short exposure photographs or high speed framing pictures. In addition, the contrast on the video pictures was poor showing only the illumination from the hot zones in front of the fuel nozzles. The flame illumination was filtered with a near ir filter for the video taping.

The optical signal from the combustor at visible wavelengths is almost entirely from emission of the luminous soot particles generated in a combusting oil flame. Wavelength spectra of this emission was taken with a scanning monochromator and a rapid scanning optical multichannel analyzer (OMA). On the OMA system the spectra of the combustor was stored on a diskette along with spectra from a standard lamp at several different lamp color temperatures. The two sets of spectra could be compared and a mean color temperature inferred.

Using a single fiber to receive the light signal from a small group of pixels at the output end of the fiberscope, we could detect a flame motion or flicker frequency due to turbulence in the combustor. The light signal from the single fiber was detected and sent to a Fast Fourier Transform Analyzer for a presentation of the frequency spectra. A peak in the spectra occurred at about 270 Hz that may be related to an acoustic resonance in the combustor. This represents a new technique that could be used to analyze the acoustics of combustors during operation. The resonances are driven by the turbulent gas or blade passing frequencies and could be deleterious to engine performance or durability.

A single optical fiber that carried argon laser light was also placed in the fiberscope probe. The fiber terminated at the viewing lens and sprayed laser light into the combustor. The backward scattering of the laser light from the fuel spray was observed and the laser beam could be seen disappearing into the combustion zone after ignition of the fuel. This technique can provide a small but very intense source of coherent light for illumination and possible future combustion diagnostic use.

In the following four sections we will discuss the program in more detail. The considerations that went into the optical and mechanical design of the viewing probe will be discussed first and then a description of the bench tests and their results will be given. A description of the high pressure

burner rig and the operation of the probe on the rig will follow next. An analysis of the spectral data taken during the combustor test will then be made; and the last section will present the conclusions of the program and discuss important aspects for future work.

2. FIBERSCOPE DESIGN

2.1 Optical Design.

2.1.1 Fiber Optics Imaging System. There are two types of fiber optic image transferring devices. One type is a rigid rod or conduit composed of tens of thousands of glass fibers fused together. The second type uses separate and unfused fibers of larger diameter forming a flexible cable. In both cases the fibers are arranged coherently; that is, the location of one fiber relative to another is maintained from one end of the cable or rod to the other. An object imaged on the end of the coherent fibers will emerge from the opposite end of the cable or conduit unscrambled.

The combustor fiberscope probe was designed with a rigid image conduit to transfer the image of the combustor flame to a position outside the burner rig. The image is then transferred with a lens to a 9 ft long flexible coherent bundle of optical fibers that transmits the image to a location outside the wall of the burner stand and into an adjoining trailer. The combustor image can then be safely viewed or analyzed with various optical instruments during combustor operation. Figure 2.1 shows a schematic of the optical system for the fiberscope and laser illuminator. The image conduit used for the probe is 20 cm long and only 3 mm in diameter, but contains 81,600 individual fibers, or 1/3 the number of picture elements of a television camera. The operating temperature limit of the conduit is that of the glass used in the fibers and is about 1000°F (540°C).

An image conduit was used in the combustor because of the higher operating temperature and smaller diameter for equivalent resolution obtainable with the conduit over a flexible bundle. The flexible bundles are bound together at each end with an epoxy compound. The resolution of the fiber bundles are in general not as good as the best obtainable resolution from an image conduit, and the operating temperature of the flexible bundles is restricted by the bonding epoxy. In addition, the flexible bundles must be well protected with a surrounding cover and be lubricated in some fashion to avoid fiber breakage. As a consequence, a flexible bundle for the combustor probe would require a larger probe diameter for the same resolution and more cooling air as compared to an image conduit. A flexible image bundle can carry an image over a much greater distance, however, without image degradation and, of course, is immune to vibration and thermal expansion problems by being flexible. A long flexible image bundle was therefore used to transfer the combustor image to a safe location away from the burner rig.

2.1.2 Viewing Lens. The viewing lens, used at the end of the probe to image the luminous burner flame onto the end of the fiber conduit, was designed using an OSLO II computer program. The OSLO program will take a given lens geometry and adjust lens parameters such as curvature, spacing and aperture size to minimize aberrations and field curvature in the image plane. We optimized a symmetric doubtlet lens composed of two identical plano-convex

OPTICAL SYSTEM FOR FIBERSCOPE AND LASER ILLUMINATOR

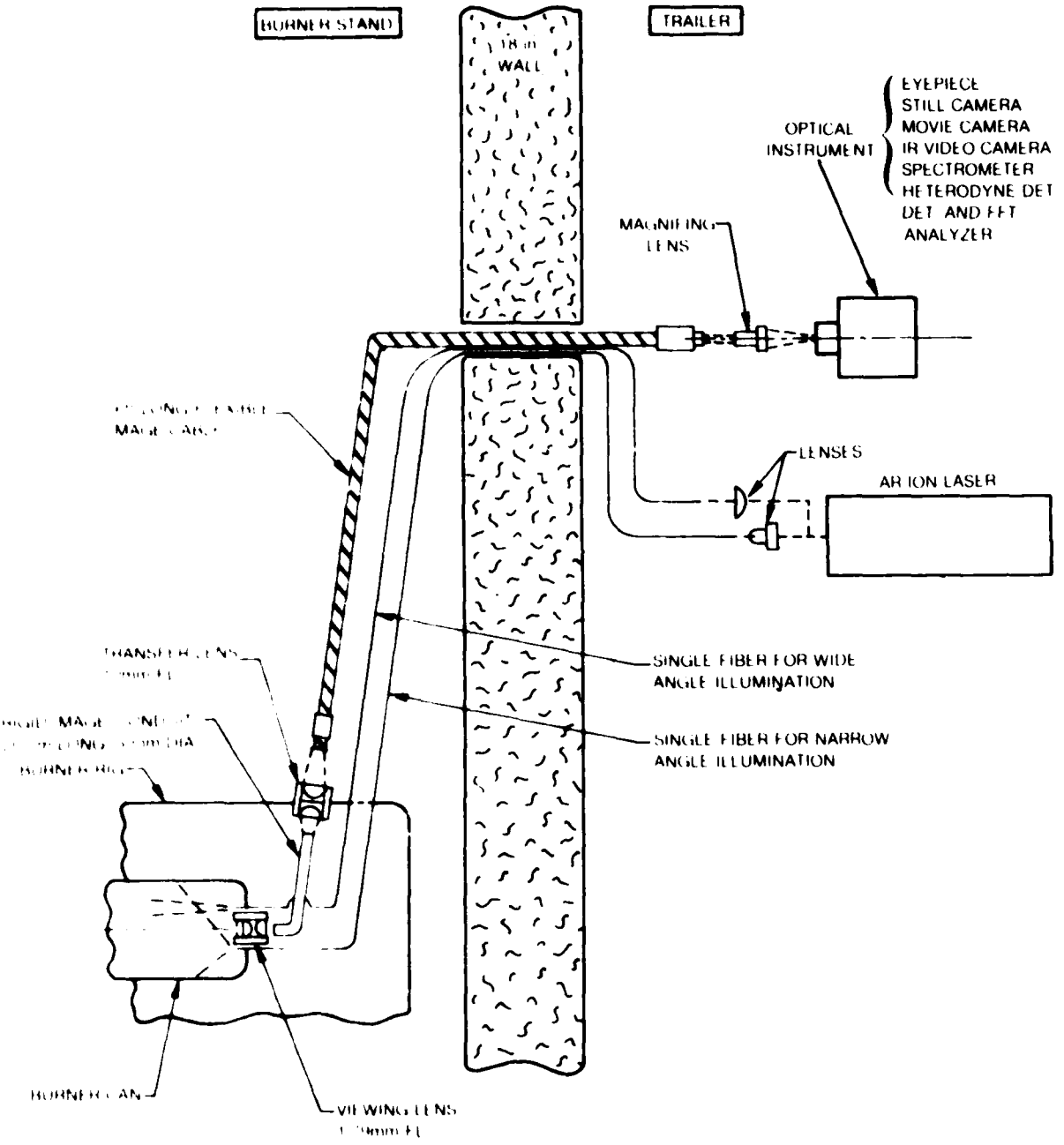

lenses with their curved sides facing each other. The field-of-view was set for 90°. Sapphire with its high refractive index produced a better lens design than fused quartz and was chosen for the lens material. Sapphire also has the advantage of a much higher operating temperature than fused quartz. The viewing lens has a 1.0 mm diameter aperture placed about 0.4 mm in front of the lens and an effective focal length of 1.79 mm. The diameter of the lenses is about 3.6 mm.

A ray tracing plot from which the sapphire lens doubtlet was designed is shown in Fig. 2.2. The focusing of parallel ray bundles at 0° (on-axis), 27°, 35°, and 45° are shown. At 45° there is vignetting of the extreme rays which reduces the transmitted intensity. For angles greater than 45°, which correspond to field-of-views (FOV) greater than 90°, the vignetting would be severe and limiting.

A magnified view of the intersection of the rays with the image plane (which is also the face of the image conduit) is shown in Figs. 2.3 and 2.4. In Fig. 2.3 the rays are on-axis and form a blur circle of 20 μm in diameter. At the full field angle shown in Fig. 2.4 the blur circle increases to an average diameter of 75 μm.

From the ray tracing results we determined the effect of the lens aperture size on the image plane blur diameter for three different viewing angles. The results are plotted in Fig. 2.5 along with a broken curve showing the blur circle from diffraction only at the aperture. From the plot (Fig. 2.5) we see that aperture sizes less than 0.4 mm would be required to make the system diffraction limited for on-axis rays. For our design we have to trade-off light gathering efficiency, which goes with large apertures, against image quality for small apertures. The resolution distance at the image conduit face, however, which is limited to about twice the separation of fibers, is 20 μm. Using the plot in Fig. 2.5, an aperature of 1 mm was chosen as the best compromise between resolution and largest aperature for light gathering power. With a 1 mm aperature the viewing system has an f-number of 1.8.

2.1.3 Image Transfer. A symmetric doubtlet lens with a focal length of 10.0 mm was used to transfer the image from the output end of the image conduit to the input end of the American Optical 9 ft long flexible image bundle (cf. Fig. 2.1). A between the lens aperature of 2 mm was required to reduce image distortion from lens aberrations. With the symmetric lens and aperture we could transfer the image with no noticeable distortion; although, there was a reduction in the image intensity by a factor of 5 with the reduced aperture. The transfer lens is positioned to give a magnification of 1.25. This magnification will match the 3.2 mm image size or the conduit of the 4.0 mm cross section of the flexible fiber bundle.

The 2 mm aperture increased the fiberscope f-number to about 10 with a corresponding decrease in light gathering efficiency. One can transfer the image efficiently from the conduit to the fiber bundle by placing the ends of

FIG 2 2

RAY TRACING FOR SAPPHIRE LENS DOUBLET

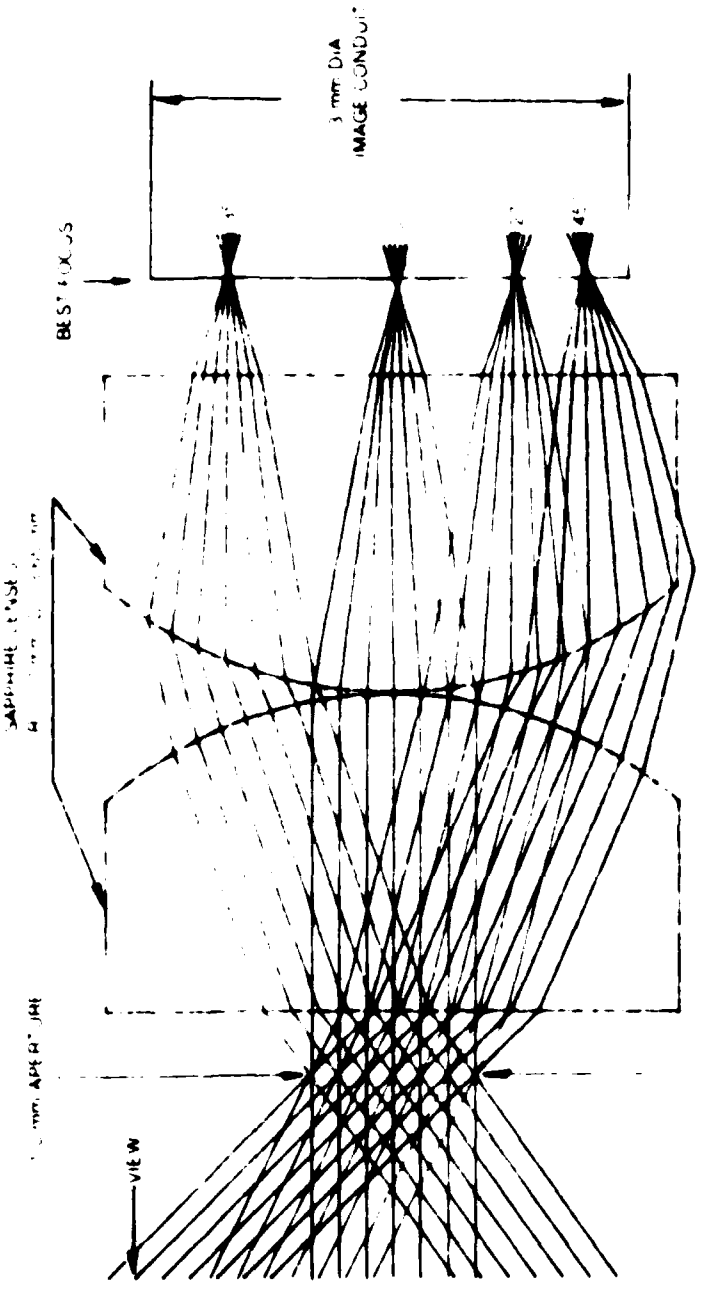

FIG. 2.3

BLUR IN IMAGE PLANE FROM RAYS ON-AXIS

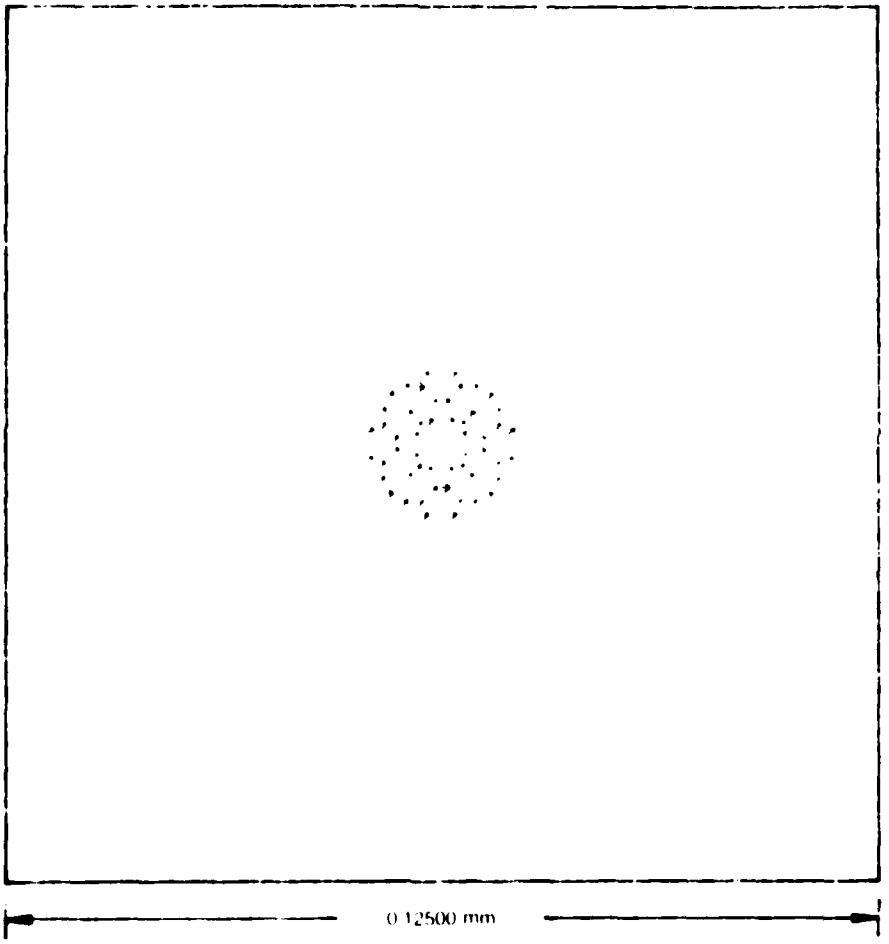

81-6-155-8

FIG. 2.4

BLUR IN IMAGE PLANE FROM RAYS AT 45° TO AXIS

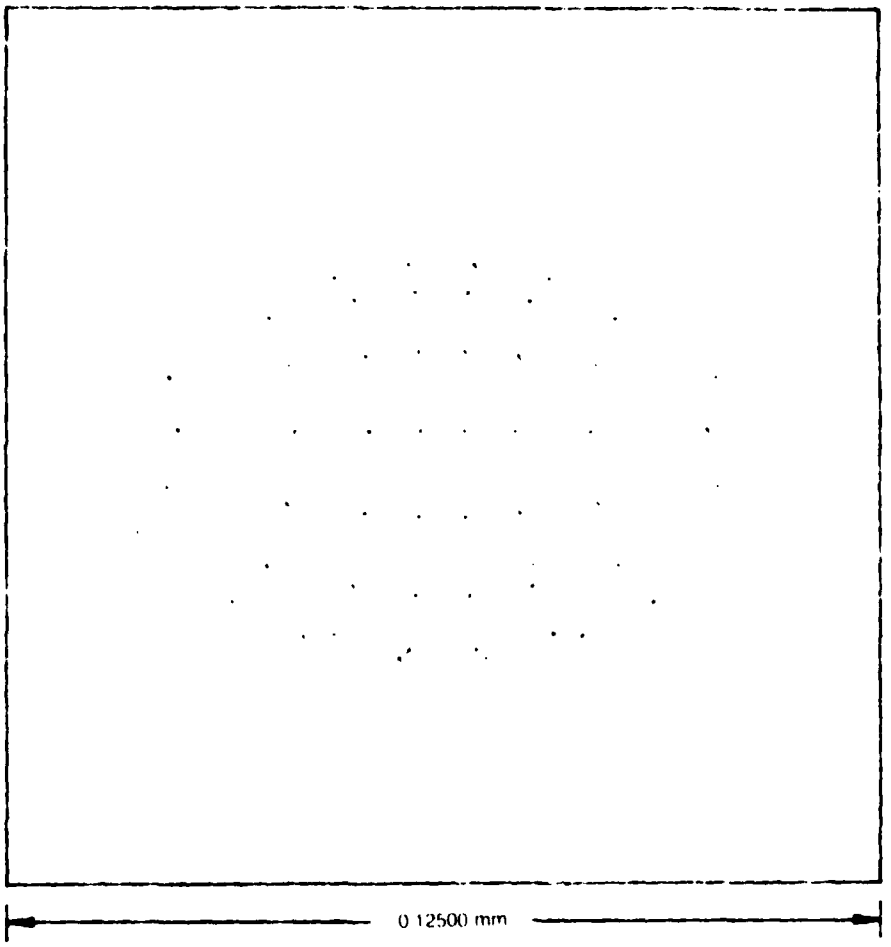

81-6 155-9

FIG. 2.5

VIEWING LENS BLUR SIZE VS. APERTURE DIAMETER FOR 3 VIEWING ANGLES

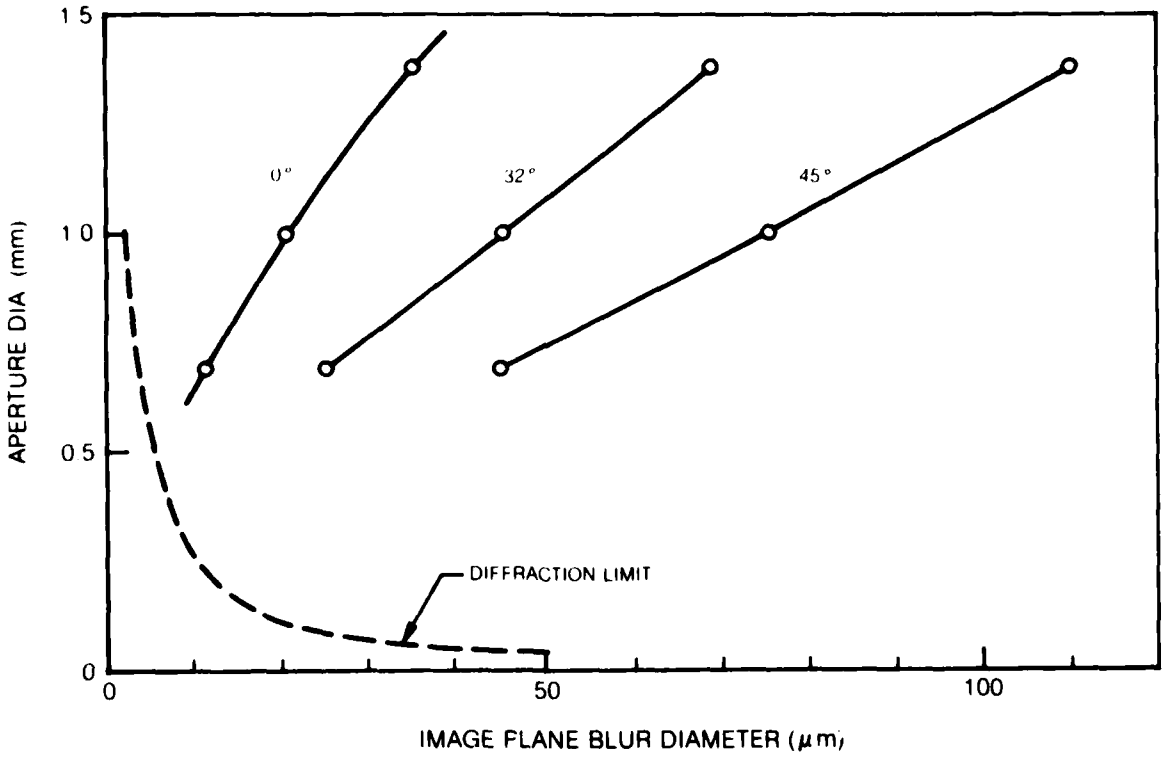

80-12-33-4

the conduit and fiber bundle in contact (butt couple). Using the transfer lens in place of butt coupling removes any change of chaffing between fiber ends and forms a convenient pressure seal between the conduit housing and the outside world. In order to take moving pictures at 5000 frames/sec, however, more light intensity was needed and the fiberscope was modified to permit butt coupling of the conduit and fiber bundle. A carefully built pressure seal was needed around the image conduit at the output coupling end. This will be discussed later.

2.1.4 Illuminating Fibers. Two single fibers were used to illuminate the viewing region with laser light as illustrated in Fig. 2.1. The fibers were .125 mm and .250 mm in diameter and were carried down the viewing probe along side the image conduit. Since and entire laser beam can be focused into a single fiber, we can transport a very bright source of coherent illumination conveniently inside the fiberscope probe. One fiber was a wide angel illuminator to view the combustion chamber and spray patterns; and the second fiber proivded a narrow angle illumination for backscattering tests. The angle of illumination can be adjusted by proper selection of fiber type and end preparation of the fiber. A narrow angle illumination can be achieved with a small lens such as a graded index lens. Space did not permit the use of a second lensing system for the narrow beam illumination, however. A low numerical aperature (NA) fiber had been made that gave an illuminating angle of only 5.6°. This fiber had a high absorption loss, however, and could only be used in short lengths of a few feet. A standard low NA, low loss communications fiber was used instead that gave an illuminating angle of 16°. A wide angle fiber could be made by producing a short taper on the end of a high NA fiber or by placing a ground surface on the end of the fiber. Both methods of fiber and treatment produced illumination angles of 180°. The tapered end fiber, however, was subject to easy breakage and was not used in the fiberscope.

2.2 Probe Design.

2.2.1 Probe Cross Section. A cross section of the viewing probe taken from the blueprint is shown in Fig. 2.6. In the figure the probe is shown attached to the burner rig wall on a 2-in diameter boss. The boss has a 1-in diameter hole that will just allow the probe to be angled through for insertion in the rig. In order to fit the probe between fuel lines and into a hole in the burner can, we had to angle it 8° forward from the center line of the boss as shown in the figure. The probe piece that extends into the burner rig and carries the image conduit is made from two halves of a 1/2-in diameter stainless steel rod. The two half sections were ball milled as illustrated in the figure and fastened together in a clamshell fashion at five positions with 0-80 screws. An enlarged view of cross section D-D where the half sections are attached is shown in Fig. 2.7. The 3 mm diameter image conduit is supported at three other positions with spring clips as shown in cross section C-C of Fig. 2.7.

COMBUSTOR VIEWING PROBE

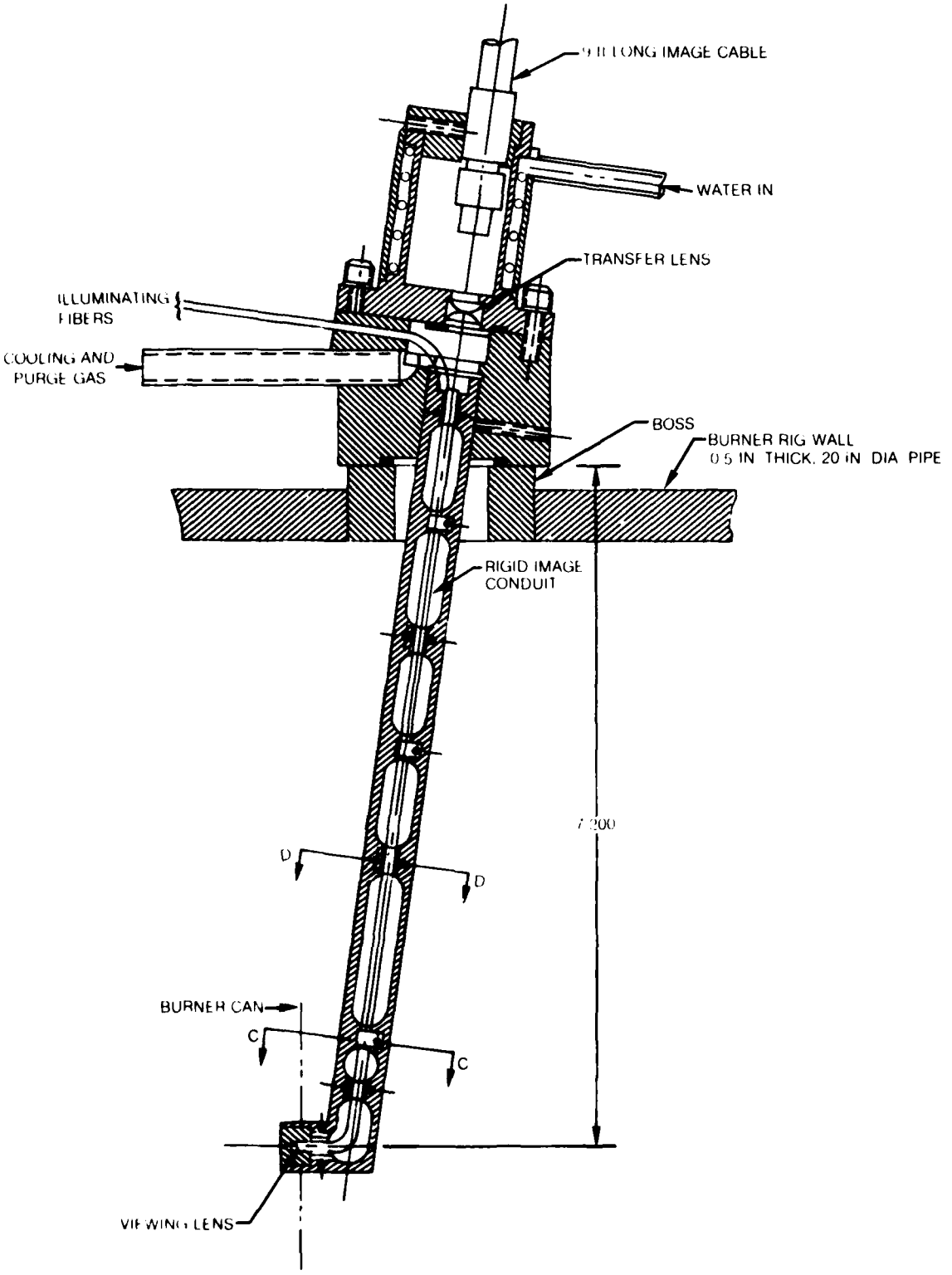

80-9-28-2

FIG. 2.7

VIEWING PROBE CROSS SECTIONS

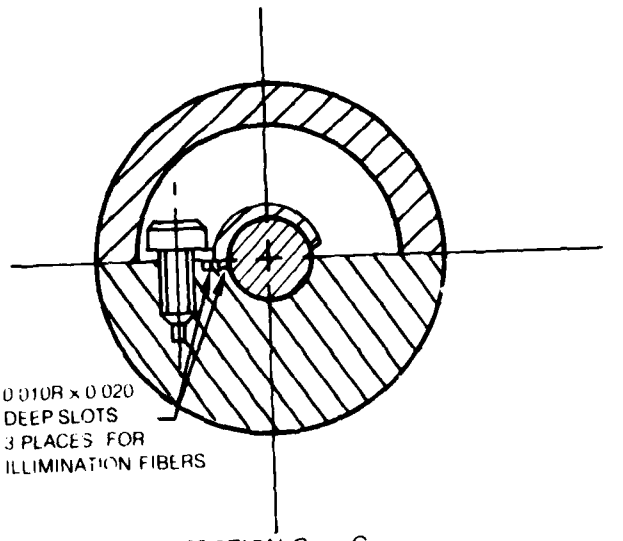

SECTION C — C
SCALE 4:1

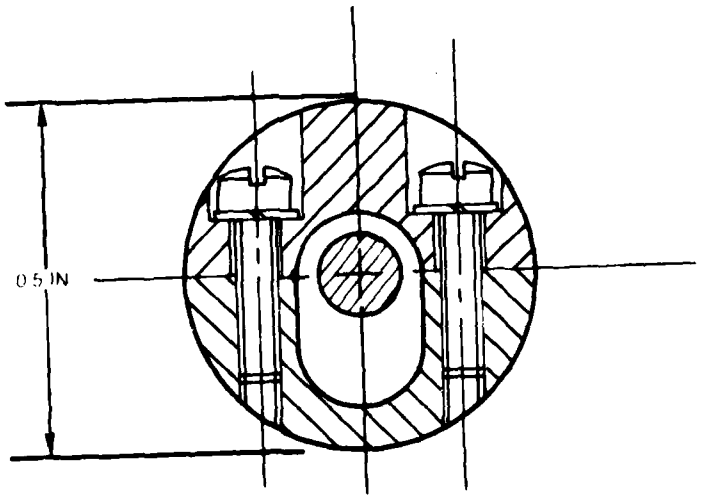

SECTION D — D
SCALE 4:1

80-9-28-3

Construction of the probe in two halves allow us the flexibility of disassembly, reassembly, replacement of the image conduit, and adjustment of the mounting forces on the conduit. Adjustment of the conduit mounts is important to allow for differences in expansion and a small amount of bending. Being able to assemble the probe in halves also permits convenient mounting of the illuminating fibers and thermocouple sensors to monitor the internal probe temperature at different positions.

2.2.2 Lens Mount. The 3/8-inch long tip end section of the probe that protrudes into the burner can is not a half shell but a continuous round piece with a threaded hole to receive the viewing lens in its holder. An enlarged view of the probe tip is shown in Fig. 2.8. The lens mount which holds the two sapphire lenses is threaded into the end piece as shown. Proper focus of the viewing lens is made by turning the threaded lens mount to adjust the lens--image conduit spacing. A series of ten holes 1 mm in diameter were drilled around the viewing lens to allow the cooling gas to escape. There are also two smaller holes, shown on the top and bottom in the end view of Fig. 2.8, with a .34 mm final diameter that hold the ends of the laser illuminating fibers.

2.2.3 Probe Mount Piece. The mounting piece that supports the probe extending into the rig with three set screws and "O" ring seals contains the cooling gas inlet and a small mechanically sealed hole for the illuminating fibers and thermocouple wires. An Advanced Products high temperature metal "O" ring is used to seal the probe mounting piece at the boss on the burner rig pipe. "O" rings elsewhere in the mount are made of silicone rubber. The top piece that attaches to the probe mount (cf. Fig. 2.6) contains the transfer lens and supports the end section of the 9 ft image cable. This piece is water cooled to avoid possible damage to the epoxied end of the fiber bundle and silicone rubber seals. The transfer lens with gasket forms a pressure seal between the two pieces. The lower chamber in which the cooling gas enters is maintained 10 to 20 psi above the rig pressure (185 psi). The upper chamber is kept at atmospheric pressure with a small bleed hole.

To achieve butt coupling of the conduit to the fiber bundle, the transfer lens is replaced by a small rod holder piece and a longer conduit is used that extends an extra 1 1/2 inches into the upper mounting piece. The conduit passes through the rod holder that makes a pressure seal to the conduit in a manner similar to a quick-disconnect vacuum connector. A tightening nut presses an "O" ring in a special "V" groove firmly around the conduit giving both a pressure seal and mechanical support.

The air mass flow in the combustor is 35 lbs/sec. This mass flow rate applies about a 2.6 pound force on the extended portion of the viewing probe in the combustor. Calculations of the bending of a cantilevered rod indicate that the probe is sufficiently stiff and that the bending due to air flow should be no more than a couple mils at the viewing lens position.

FIG 2.8

VIEWING LENS ASSEMBLY

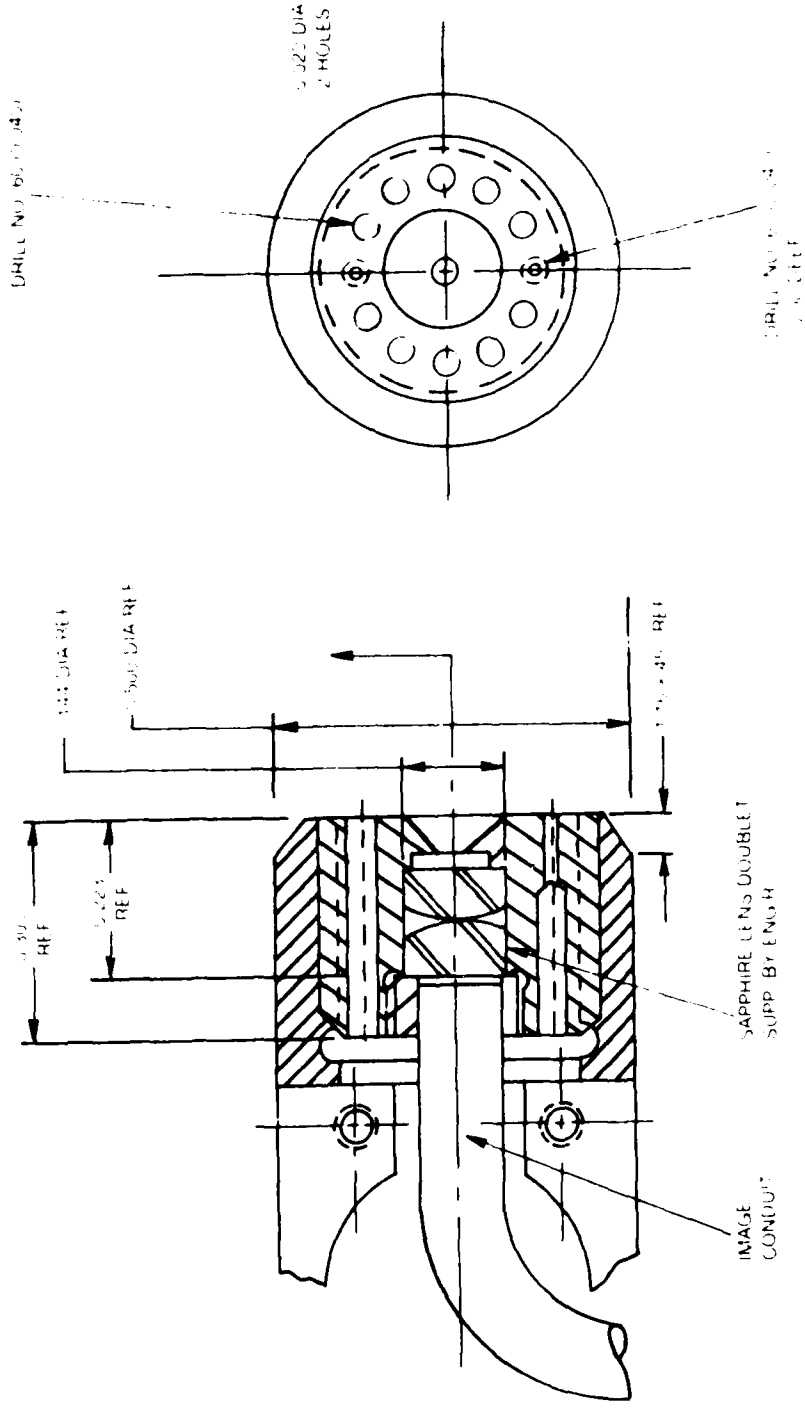

81-6-155-6

2.2.4 Photographs of Probes. A photograph of the assembled fiberscope is shown in Fig. 2.9. The probe has an 82° bend at the end to view downstream into the combustor can. Cooling air enters the probe mount in the 3/8 inch diameter tube on the right-hand side, makes it way down the length of the probe, and emerges through the series of holes that can be seen surrounding the viewing lens aperture at the probe tip. The laser illuminating fibers enter a sealed port on the side of the probe mounting piece shown in Fig. 2.9 and emerge at two very small holes near the cooling holes. The 9 ft long flexible image cable can be seen leaving the top of the unit. Figure 2.10 shows a photograph of the fiberscope disassembled into its four major components. The fiber conduit and its three small clamps can be seen in one of the probe half shells. The viewing lens holder with the cooling hole ports is threaded into the end of the probe to allow for a fine focus adjustment. The transfer lens can be seen at the bottom of the top piece in the photograph. This piece is water cooled and holds the flexible image conduit that is inserted in a hole on the top side.

2.2.5 Probe Cooling and Purging. In the combustor rig the fiberscope probe is subjected to inlet gas temperatures that range up to 380°C, and the viewing end of the probe that faces the combustion zone will receive additional heat loading from the radiant heat of the flame. The end of the probe is also subject to soot deposition from recirculating combustion gases. In addition, if unburn fuel condenses on the end of the probe either burning or carbonizing can take place to add further to the build up of carbon. To reduce the heat loading on the probe and eliminate soot or carbonizing deposits that cover the viewing lens a steady flow of nitrogen was driven through the probe at about 20 lbs/hour and exhausted through the ten holes surrounding the viewing lens. Two of the holes on opposite sides of the lens were blocked off and small channels cut to direct some of the nitrogen onto the outside surface of the lens. The diverted flow was sufficient to keep the lens soot free as will be shown later.

Control of the mass flow rate of cooling air through the probe is accomplished with the use of a sonic flow constrictor that has an orifice diameter of 0.52 mm. As long as the downstream pressure is significantly less than the pressure applied upstream of the constrictor, the mass flow rate depends only on the applied pressure. Flow test measurements we performed gave the mass flow, $\dot{m}$, in lbs/hrs through the constrictor as

$$\dot{m} = .028\ P$$

where P is the inlet pressure in psig. A moving vane flowmeter with a fiber optic pickup for remote flow monitoring was also placed between the flow constrictor and probe inlet. Calculations and measurements were made to estimate the cooling ability of the gas flow through the probe. These will be discussed in section 3.3.

FIG 2.9

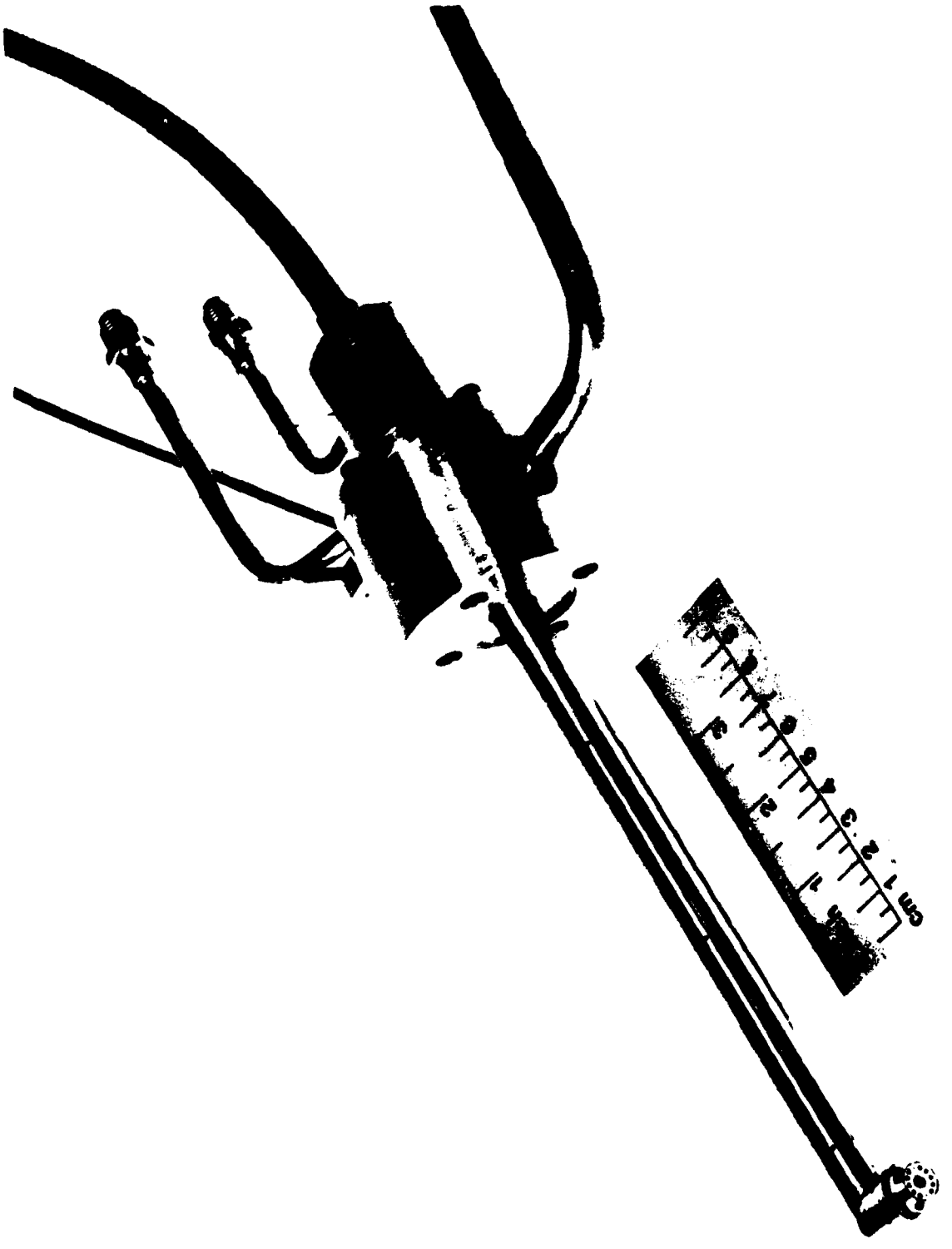

ASSEMBLED VIEW OF FIBERSCOPE

80-368-B

80-12-33-10

FIG 2 10

DISASSEMBLED VIEW OF FIBERSCOPE

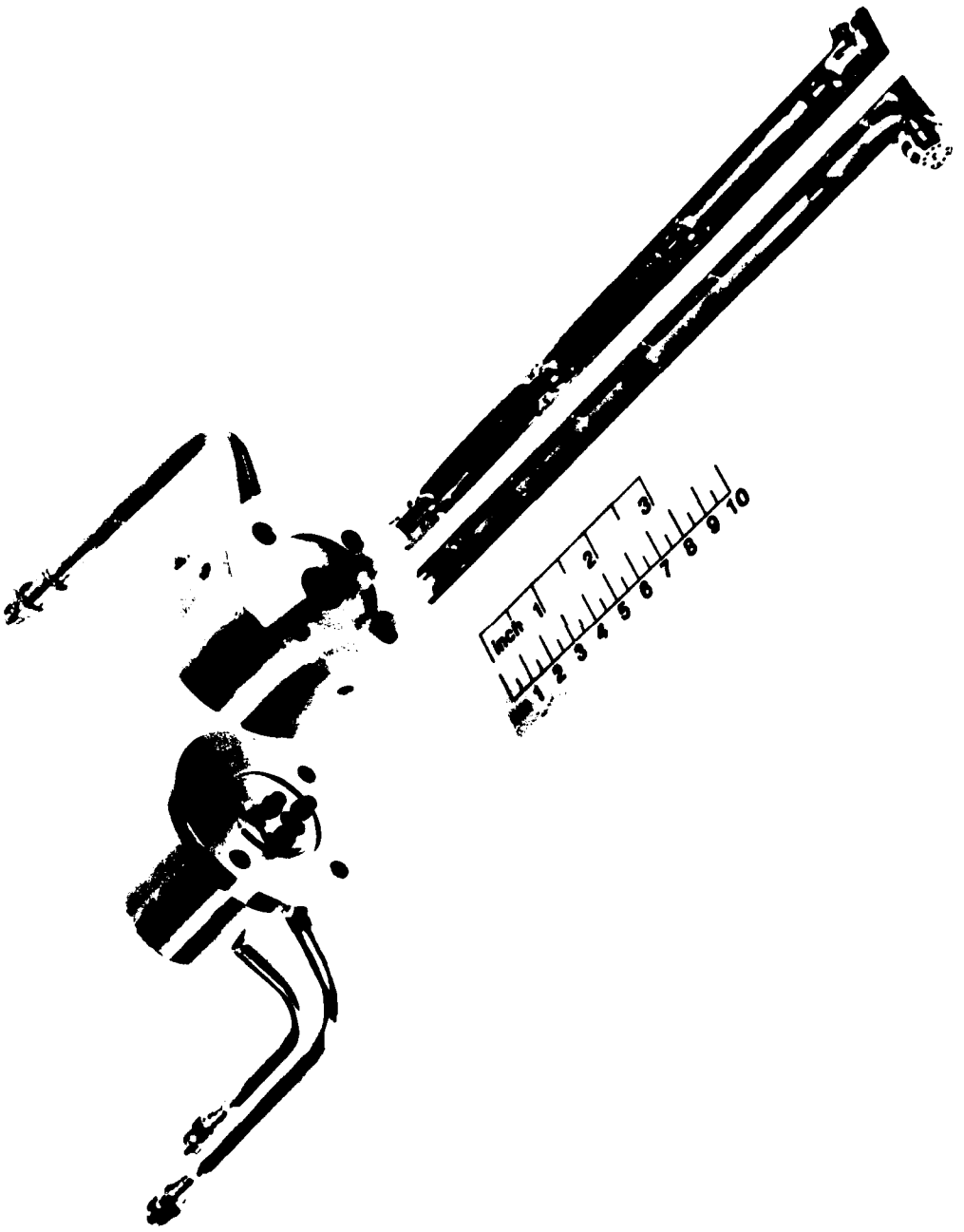

80-368-D

80-12-33-9

3. BENCH TESTS

3.1 Optical Viewing.

3.1.1 Fiberscope Resolution. The fiberscope viewing system was set up on the bench to determine the image quality with different image conduits, lenses, and couplings between the conduit and fiber bundle. An illuminated USAF resolving power chart that shows a stepped series of three bar patterns was used as a viewing object.

Theoretically, the maximum resolution of a fiberscope through which an object at a distance D from the viewing lens is being observed is given by:

$$\gamma_0 = F/[2d(D-F)] \doteq F/2dD \text{ for } D \gg F$$

where F is the focal length of the viewing lens and d the distance between individual fiber elements in the bundle or conduit. When the object distance is twice the focal length (D=2F) we have a magnification of 1 and the resolution becomes 1/2d which represents the resolution of and object at the face of the fiber bundle or conduit (Ref. 5). The above result is for a uniformly closepacked bundle. The resolution can be worse if the fibers are not uniformly packed or there are a number of broken or weakly transmitting fibers.

For the imaging fiber conduits and bundles that we are using d equals 10 μm and the resolution of a object at the conduit face (or a distance 2F away from the viewing lens) is 50 lines per mm. When we increase the object distance, D, the resolution of the object decreases since we are demagnifying the object onto the conduit face. The amount of demagnification in the object plane depends on the field-of-view (FOV); and, for a simple lens, the FOV is just equal to twice the angle whose tangent is the ratio of the conduit radius divided by the conduit face to lens distance. For objects whose distance is much greater than the lens focal length the FOV is just:

$$FOV = 2 \tan^{-1} (r_c/F)$$

where r_c is the conduit radius. Basically, lenses with focal lengths near the size of the fiber bundle diameter will have large FOVs with low resolution; and lenses with focal lengths much larger than the bundle diameter will have narrow FOVs and higher resolution. In addition, the short focal length lenses will have a large depth of focus (range over which objects remain in focus) and the long focal length lenses a much shorter depth of focus. There is a trade-off, then between high resolution with small depth of focus against wide FOV with large depth of focus.

The resolution for the fiberscope discussed above was for viewing a stationary object. As discussed by Kapany in Ref. 5, if the object is moving

relative to the fiber bundle, then the mosaic pattern of the bundle array is to a certain degree eliminated. This improves the resolution by a factor of about 2. This effect gives an apparent improvement in resolution when observing the high speed motion pictures of the moving flame as compared to an examination of a single frame.

We found that the resolution of the image conduits varied considerably with manufacture and with the different batches from the same manufacturer. The variation in resolution depended on the number of broken or weakly transmitting fibers. In short length of 2 to 3 inches the conduit resolution was usually the theoretical value expected. In longer lengths, however, of 7 to 12 inches a large number of weakly transmitting fibers became dark, the image became snowy and the resolution could be degraded by a factor of four. In many cases the weakly transmitting fibers were at the boundary of the second draw of a multidraw process. In this case a second much larger mosaic pattern is superimposed on the basic pattern. Image conduits from some companies were acceptable and gave nearly the theoretical resolution expected at the longer lengths required.

When we couple from one fiber optic imaging device to another, as we did in going from the image conduit to the flexible fiber bundle, only a slight degradation of about 10 percent in resolution is expected (Ref. 6). This was observed to be the case and the completed fiberscope with the transfer lens or butt-joined fibers gave nearly the expected resolution. Figure 3.1a shows a photograph of the USAF resolution test pattern taken through the fiberscope. The test pattern was placed 10 cm from the viewing lens. The corresponding test pattern and resolution values in lines per mm are shown in Fig. 3.1b. In the photograph we can just resolve group-1, element 6. This corresponds to .891 lines/mm. The viewing lens focal length is 1.79 mm and the individual fiber spacing on both the conduit and the flexible fiber bundle was about 10 μ. Therefore, the expected resolution is .895 ℓ/mm. The flexible fiber bundle had an additional pattern from a grouping of 16 individual fused fibers. A few of the fiber rows were not well aligned causing a shearing of the object. This can be seen, for example, in the vertical bars in group-2, element 1. Additional broken fibers appeared as the fiberscope was handled around the combustor rig.

Figure 3.2 shows a view through the fiberscope of a 1 inch square array of lines at 10 cm from the lens. From this view one can easily see the barrel distortion of the viewing lens. This type of distortion is common with wide angle lenses when a large field-of-view is compressed into a small image size. The largest FOV from the photograph is roughly 82°. A more practical FOV where the image remains discernable is about 75°.

3.1.2 Wavelength Transmission. An imaging fiber bundle typically transmits over a wavelength range between 0.40 μm to 1.64 μm at the 10 percent transmission points as given by Siegmund (Ref. 7). We measured the transmission function of the combustor fiberscope over the wavelength range of 0.45

(a) RESOLUTION TEST PATTERN THROUGH FIBERSCOPE

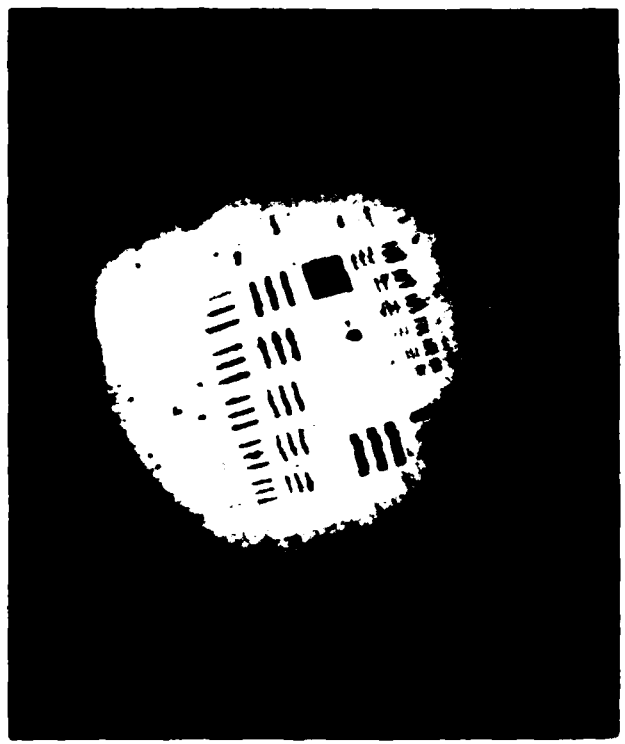

(b) VALUES FOR STANDARD USAF 1951 RESOLUTION TEST PATTERN (LINES PER MILLIMETER)

ELEMENTS	GROUPS					
	-2	-1	0	1	2	3
1	0 250	0 500	1 00	2 00	4 00	8 00
2	0 281	0 561	1 12	2 24	4 49	8 98
3	0 315	0 629	1 26	2 52	5 04	10 1
4	0 354	0 707	1 41	2 83	5 66	11 3
5	0 397	0 794	1 59	3 17	6 35	12 7
6	0 445	0 891	1 78	3 56	7 13	14 3

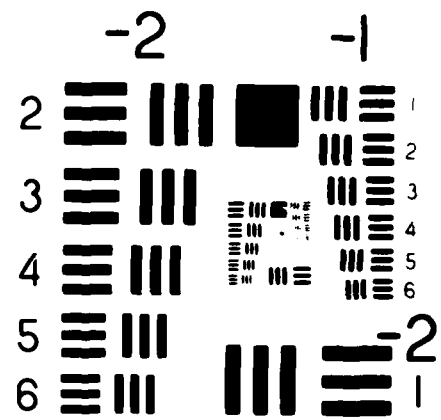

81 6 155 5

VIEW OF SQUARE PATTERN ARRAY THROUGH FIBERSCOPE

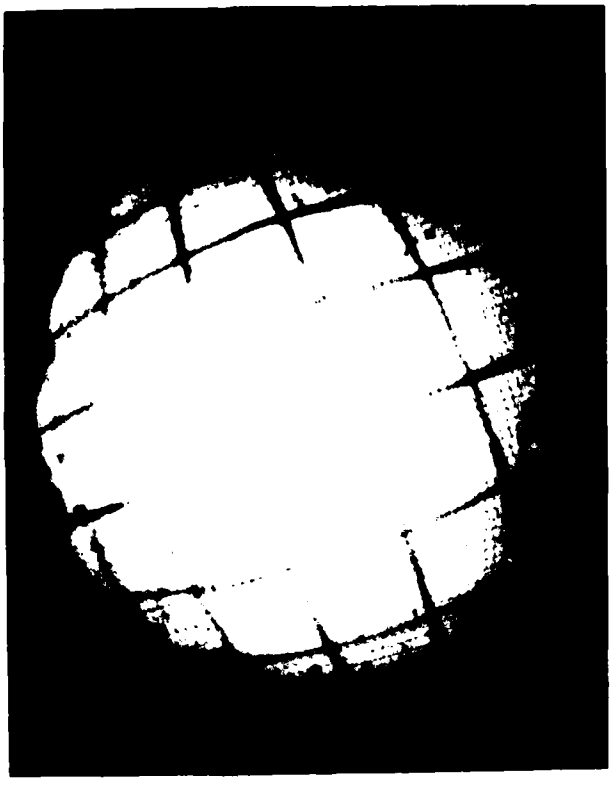

80-12-33-2

μm to 1.2 μm, which was the limit set by the photodiode detector on our scanning monochromator. The transmission function includes the transmission of the lenses, imaging fiber conduit and 9 ft bundle, and surface reflection losses.

The wavelength transmission of the fiberscope was measured with a scanning monochromator and chart recorder. We first measured the emission spectrum of a standard tungsten ribbon lamp run at 1800°C. The fiberscope was then interposed between the lamp and monochromator and the spectrum of the lamp again recorded. The light collection angle of the monochromator was kept about the same in each instance and appropriate filters were used to block the second order diffraction in the monochromator when necessary. The measurement of the lamp spectrum with and without the fiberscope gave a relative transmission over the wavelength spectrum measured. With the use of a small He-Ne laser we were able to obtain in a similar measurement the absolute transmission at the 0.633 μm wavelength. The data at the other wavelengths was then normalized to the 0.633 μm value to produce the curve in Fig. 3.3. The fiberscope transmission in the visible wavelength was only 3 to 4 percent with the lens coupling between the fiber conduit and bundle and increased to 16 to 19 percent for butt coupling of the fiber components.

In order to obtain exposure value estimates, photographs of the standard lamp were taken through the fiberscope with a 35 mm camera. A 50 mm camera lens was used with four extenders totaling 40 mm distance. With the extenders we made a 0.9 magnification image of the output end of the 9 ft fiber bundle on to the film. The resolution of the film is 50 to 100 lines/mm so there should be no significant loss of image resolution. The lamp was run at temperatures of 1500°C, 1800°C, and 2000°C to simulate expected flame temperatures. Several exposures were taken at the different lamp emission temperatures with Ektachrome 400 ASA film. The film was pushed one stop in development giving it an effective ASA of 800. Shutter speeds of 1/1000 and 1/2000 sec gave weak exposure at 1500°C and good exposures at 1800°C and 2000°C. These shutter speeds were also found to be adequate for the combustor view as expected. The exposure values were measured with the lens coupling between the fiber elements. With butt coupling we would have only one fifth the exposure value; that is, we should be able to run at shutter speeds of 1/5000 sec to 1/10,000 sec which is required for the high speed motion pictures.

3.1.3 Angular Transmission. The angular sensitivity of the fiberscope to received light was measured with a small light source placed at a constant radius but at different angles in the object fields of the fiberscope. The light signal transmitted through the fiberscope was photodetected and recorded for the different angular positions. A sufficiently sized light source was used so that several individual fiber elements in the image conduit were illuminated and a discontinuous jump as the light spot moved over the fiber elements was avoided. Figure 3.4 shows the angular distribution pattern. The half power points occur at 35° and -40°. These results are for lens coupling of the fiber imaging components. With butt joined components the results are very similar. The reason for the double lobed structure is not fully understood.

WAVELENGTH TRANSMISSION SPECTRUM OF FIBERSCOPE

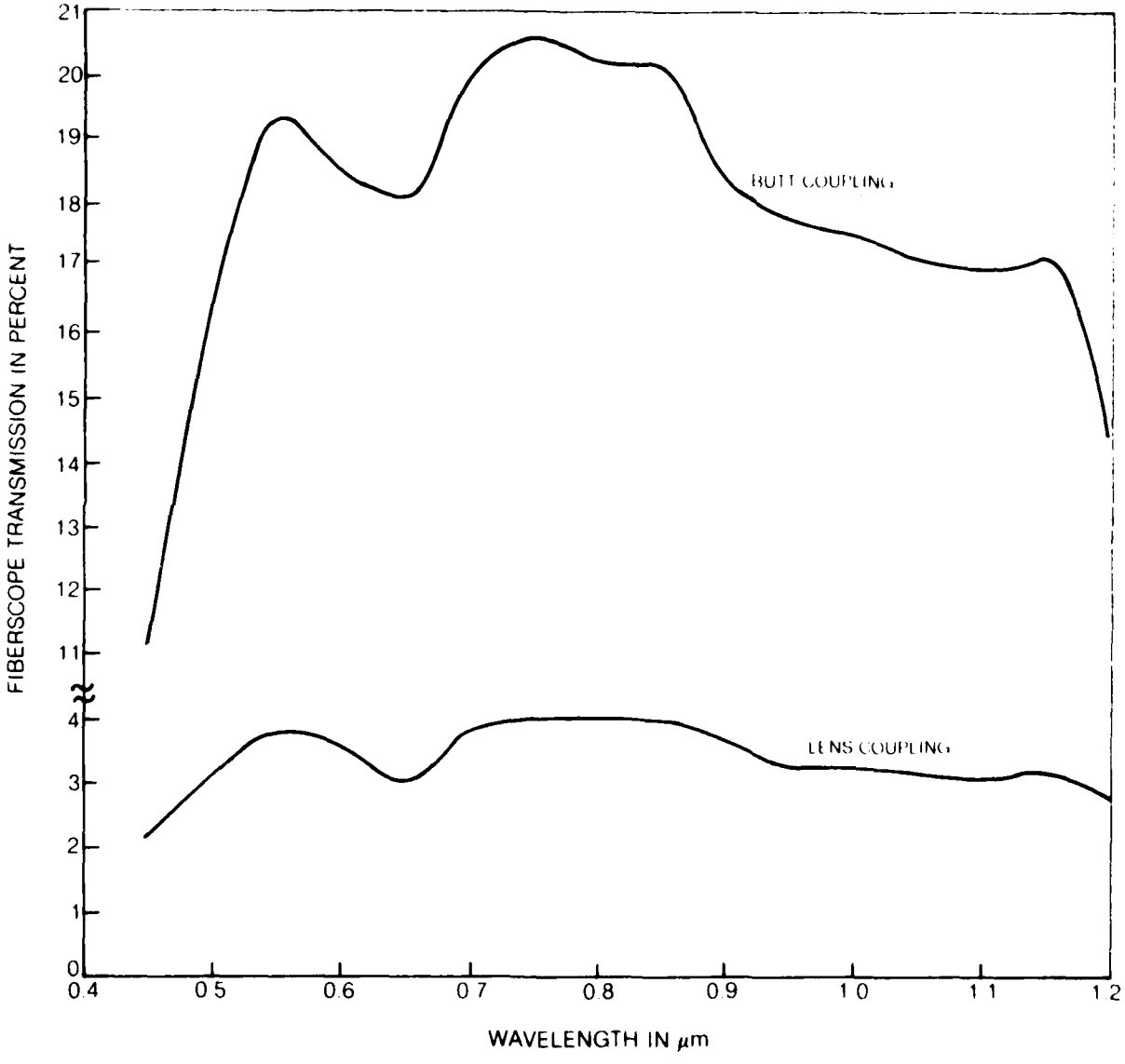

81-6-155-3

FIG. 3.4

ANGULAR SENSITIVITY OF FIBERSCOPE

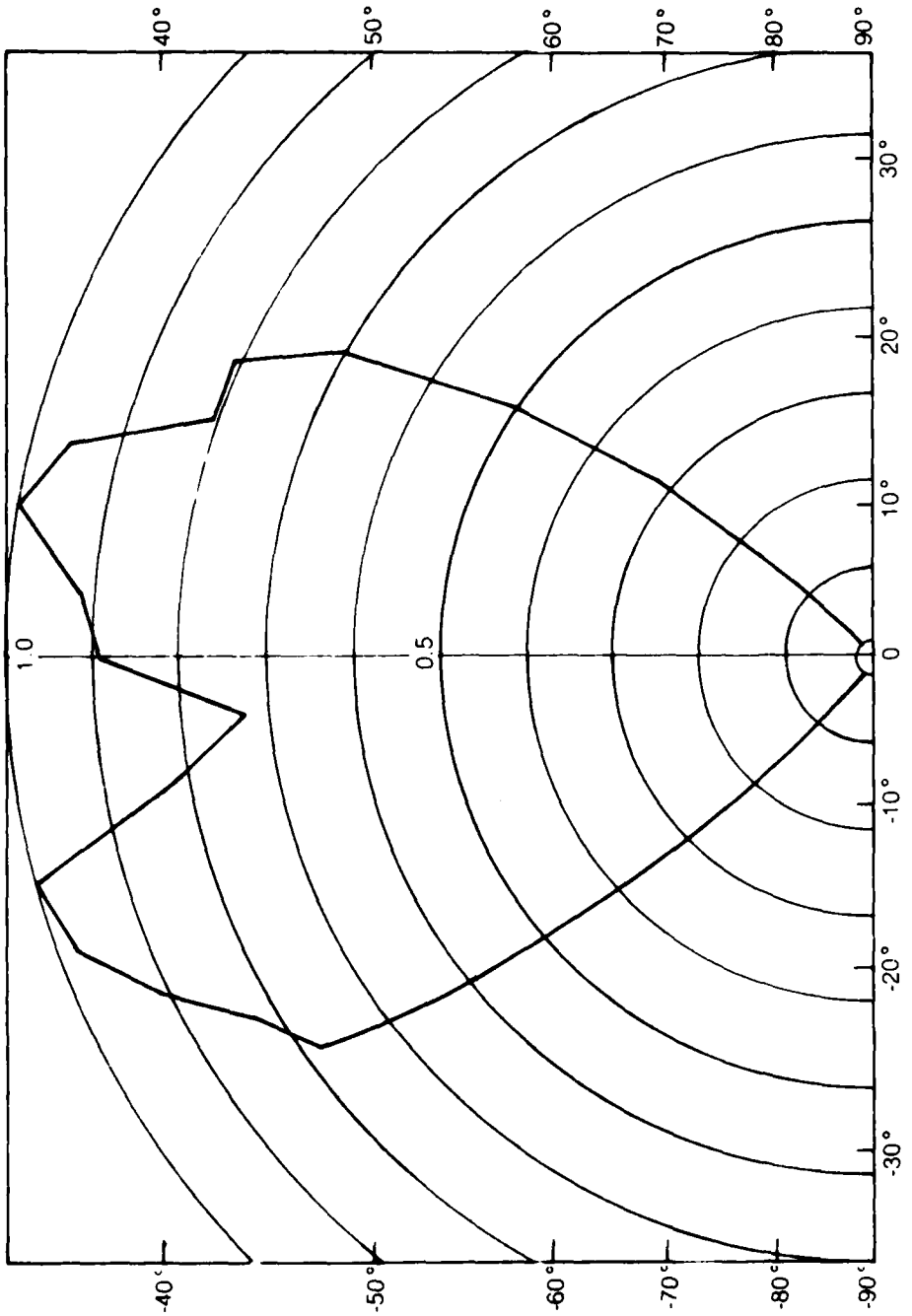

81-6-155-4

3.2 Pressure, Temperature, and Vibration Tests. A small bench rig was constructed using a standard 4 inch id, 300 psi pipe elbow. The rig was used to test the assembled fiberscope for ruggedness and ability to maintain image quality at the pressures, temperatures, and possible vibrations expected in the burner rig. Figure 3.5 shows a half scale cross section drawing of the fiberscope mounted in the pipe elbow rig. A slow flow of compressed air at 200 psig enters the elbow from the connector on the top flange next to the fiberscope mount. The air flows through the connector and into a ceramic tube with an electrical resistance heater where it is heated and discharged across the end of the fiberscope, as shown in the figure. The temperature of the gas, measured with a thermocouple probe placed near the fiberscope was set for 520°C. An exhaust port with a flow constricting value to control the pressure was placed on the flange at the other end of the pipe elbow. A screen with the words "FIBER OPTICS" was also placed on the end flange. The screen, 25 cm away from the probe, was illuminated in the sealed pipe with the laser illuminating fibers from the end of the probe. We could easily monitor the screen through the fiberscope during bench testing.

In the course of heating and pressurization of the fiberscope we also vibrated the bench rig with a motor driven eccentric load. The rotation rate of the motor was varied over the course of the tests from 0 to 7200 rpm giving vibration frequencies from 0 to 120 Hz. At certain frequencies the bench rig and the platform to which it was mounted resonated giving rise to increased vibration amplitudes. The fiberscope was tested for over four hours at the higher pressures and temperatures and vibration loadings. At no time during or after the tests was the image through the fiberscope distorted or degraded by vibrations or high temperatures and pressure imposed on the fiberscope.

3.3 Probe Cooling. Due to the complicated geometry of the probe, the exact amount of cooling gas flow required to reduce the probe temperature a certain number of degrees cannot be calculated easily. We can estimate the effect of the cooling gas, however, by making a calculation of a simplified model and taking measurements with an external heater on the probe.

If the outside surface of the probe is held at a constant temperature by the incoming hot gas, heat will transfer through the probe walls and be carried away by the cooling air flowing through the probe. In this way we can reduce the temperature of the fiber conduit and viewing lens assembly. The heat transfer through the wall of a cylinder of conductivity k with inside radius r_1 at temperature T' and outside radius r_2 at temperature T_s and length dz is

$$dQ = 2\pi k(T_s - T') \, dz/\ell n(r_2/r_1) \qquad (1)$$

Heat transfer from the inside surface to the gas at temperatures T is

FIG. 3.5

BENCH TEST RIG

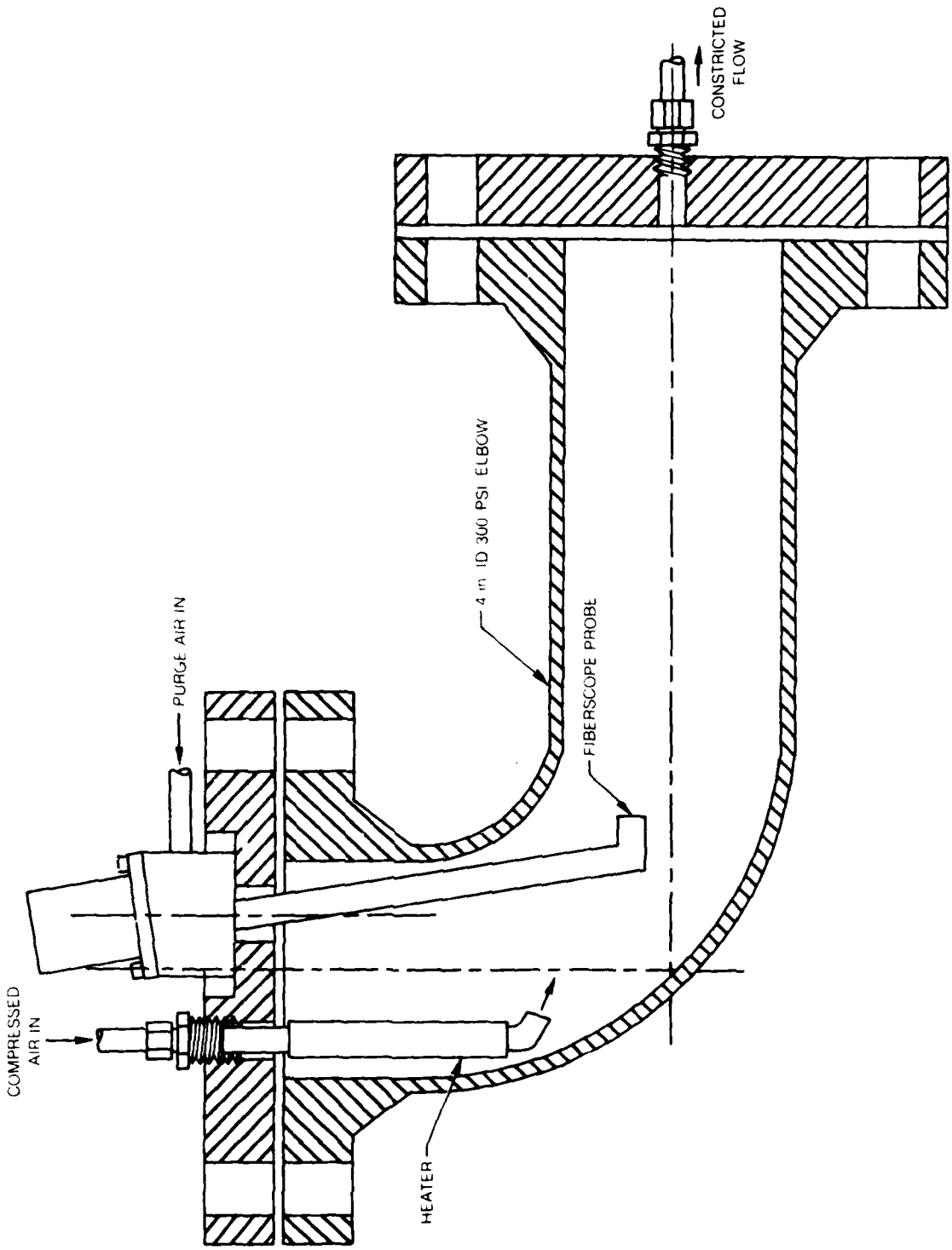

80-9-28-4

$$\dot{dQ} = 2\pi h\, r_1 (T'-T)\, dz \qquad (2)$$

where h is the transfer coefficient to the gas. We can eliminate the inside wall temperature, T', from Eqs. (1) and (2) and equate the heat flow into the cylinder to the heat carried out of the probe section dz by the flowing gas. We then get

$$c\, \dot{m}\, dT = 2\pi r_1\, h\, dz\, [(T_s-T)/(1+\alpha)] \qquad (3)$$

where c is the specific heat of the gas and

$$\alpha = h r_1\, \ln (r_2/r_1)/k$$

Integration of Eq. (3) over the length of the probe and from inlet gas temperature to outlet gas temperature gives an expression for the ratio of the exhaust gas temperature to the outside surface temperature of the cylinder wall, namely,

$$T_{out}/T_s = 1 - e^{-\gamma/\dot{m}}\, (T_s-T_{in})/T_s \qquad (4)$$

where

$$\gamma = 2\pi r_2 hL/C(1+\alpha)$$

The outside surface of the fiberscope probe was heated with an electrical resistance heater tube and insulation was placed around the probe. The temperature of the probe surface and exiting cooling gas and mass flow rate were measured. The wall thickness of the probes varies considerably along the length of the probe. Since the geometrical factors are contained in the quality of γ, Eq. (4), should represent the approximate functional dependence on mass flowrate for the fiberscope as well as for a cylinder. Measurements taken on the fiberscope of T_{out}/T_s for different mass flows are shown in Fig. 3.6. The solid curve represents Eq. (4) with $\gamma = 4.5$.

If we consider the burning fuel zone a black body emitter at 1600°C the radiant intensity would be 68 watts/cm^2. Since the probe is upstream and separated from the surface of the burning fuel by several cm, the emissivity of the luminous combustion is less than unity, the reflectivity at the surface of the probe face a significant fraction of unity; only a portion of the 68 W/cm^2 black body radiation would irradiate the 1 cm^2 surface area of the probe face. The actual position, size, and emissivity of the combustion zone and the reflectivity of the probe face in the hot oxidizing environment are not precisely known. A very rough estimate would allow for at most 32 watts or 8 cal/sec of incident radiant power to heat the end of the probe. At

COOLING CURVE

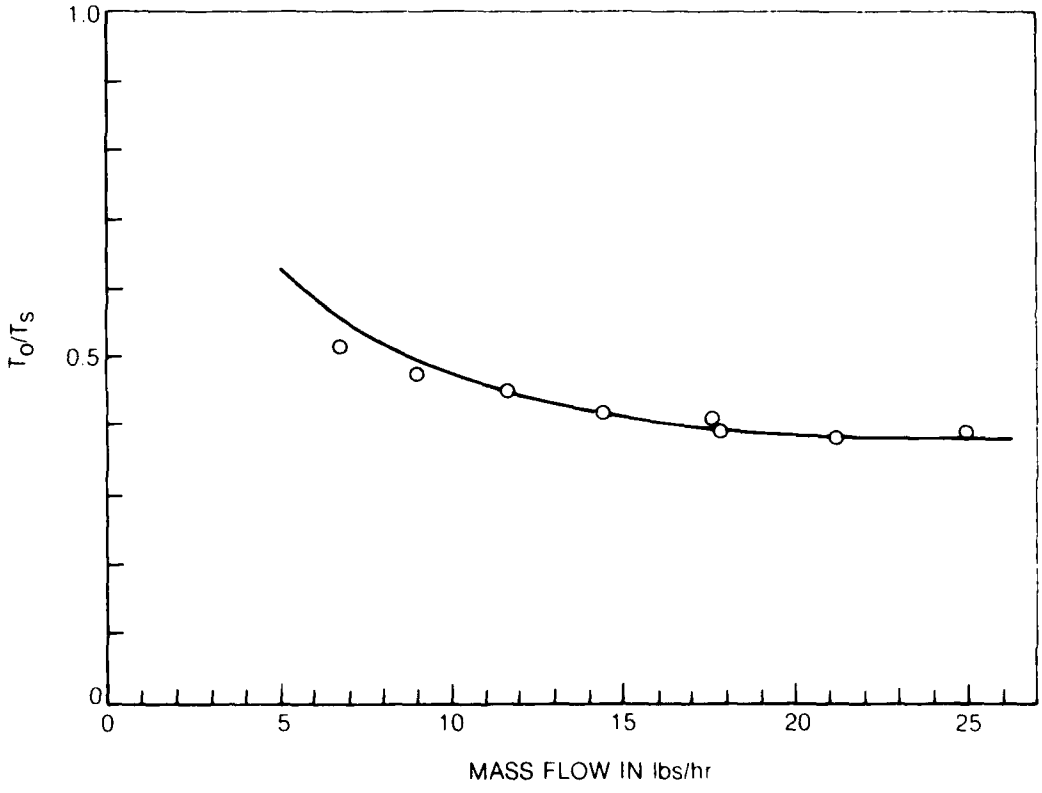

81-6-155-2

20 lbs/hr the cooling gas would have to raise its temperature by 13°C at the probe tip to carry away the additional radiant heat loading. The corresponding surface temperatures at the probe face, however, would have to be higher than the gas temperature to transfer the required heat in the short distance at the end of the probe. The bench tests could not possibly reproduce the radiant heating from the burner flame on the tip end of the probe.

A mass flow rate of 20 lbs/hr was maintained through the fiberscope during operation on the combustor rig. For operation on the rig the factor $(T_{in})/T_s$ in Eq. (4) would be about .94, and the nitrogen gas temperature should raise to a temperature that would be about 25 percent of the ambient combustor inlet temperature. This temperature rise and gas flow would carry away 57 cal/sec of heat. The gas temperature would also rise an additional small amount at the probe tip from the radiation heating.

4. HIGH PRESSURE COMBUSTOR TESTS

4.1 High Pressure Burner Rig. The fiberscope was tested on the Research Center's FT4 single can combustor test facility. This facility was designed to represent a full scale, 1/8 sector (single can) of an FT4 combustor. The FT4 is a ground based gas turbine engine that has a free turbine to deliver shaft horsepower. The engine has eight individual burner liners (or cans) around the turbine annulus. The combustor test facility was designed to simulate the actual operating conditions and air flow distribution for a single burner can.

The air flow to the combustor rig is supplied by a large tank of compressed air that is initially filled to a pressure of 400 psig. The rig operates in a blow-down fashion for a period of time that depends on the rig pressure. A backpressure valve on the exhaust controls the pressure in the rig, and a vitiation heater, using propane, preheats the air before entering the diffuser and combustor sections. Only a small fraction of the oxygen is depleted by the vitiation heater. Figure 4.1 shows a drawing of the test rig and its various components. The rig was instrumented with smoke probes, thermocouple rakes and various pressure, flow, and temperature monitors. In addition, the rig could be assembled and disassembled for easy access.

A side cross sectional view of the diffuser and combustor sections of the test rig is shown in Figure 4.2. The combustor can (or liner) is a 10 inch ID by 18 inch long annular can with a 3 inch diameter by 11 inch long reentrant tube to bring mixing and dilution air into the center of the can. There are six fuel nozzles placed around the center cooling tube as shown in the end view of Figure 4.3. Figure 4.3 also shows the 45° annular segment wall, used to simulate the engine air flow.

The combustor rig was run in two primary modes for the viewing tests. In the full power or 20 MW mode, inlet air temperature and pressure were set at 379°C and 183 psig with an air flow rate of 31.6 lbs/sec. Number 2 fuel oil was burned in the combustor and the fuel flow rate to the six nozzles was 1656 lbs/hr. In the full power mode, the burner operation could be sustained for a little more than 5 min.

The second mode of operation was at half power or 10 MW. Under this condition, the inlet gas temperature, pressure, and flow were 309°C, 135 psig, and 25.4 lbs/hr. The fuel flow was set for 996 lbs/hr. At half power the rig could run for more than 11 min.

For safety reasons, personnel are not allowed in the burner stand when the combustor rig is in operation. The rig is close enough, however, to an outside wall to allow the 9 ft long fiber bundle to go between the fiberscope

FIG. 4.1

FT-4 SINGLE CAN COMBUSTOR TEST FACILITY

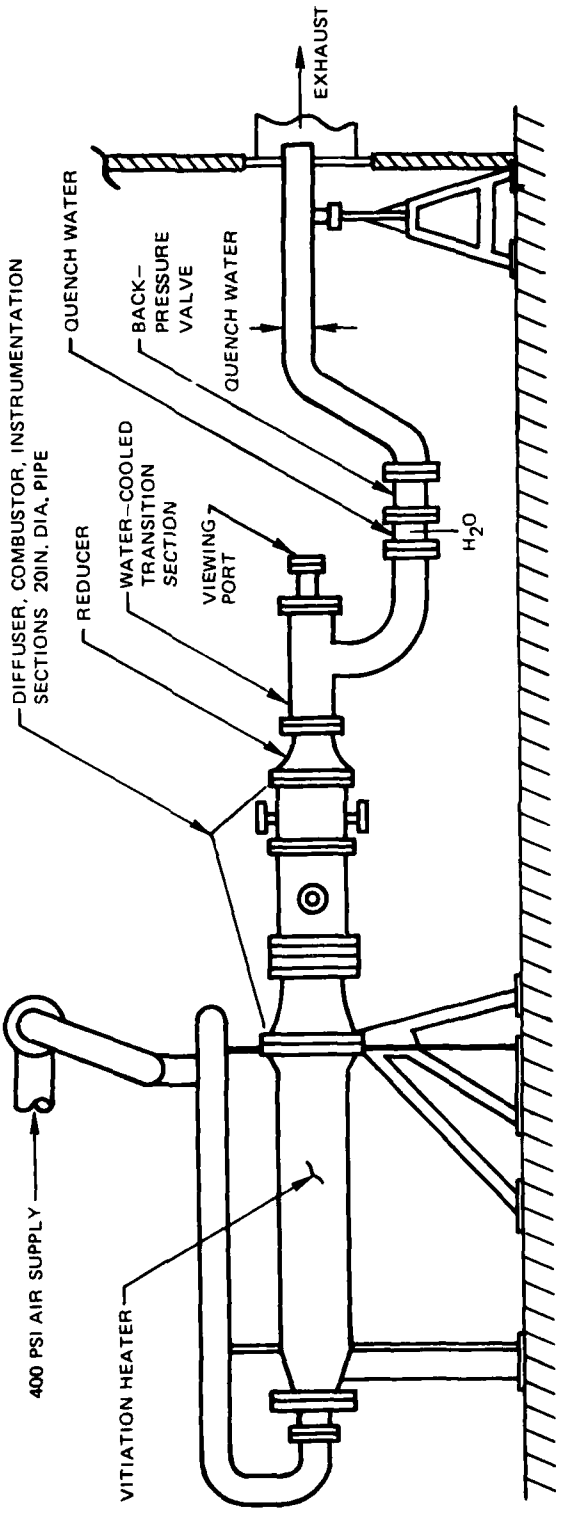

79-04-104-4

FIG 4.2

FT4 TEST SECTION SIDE VIEW

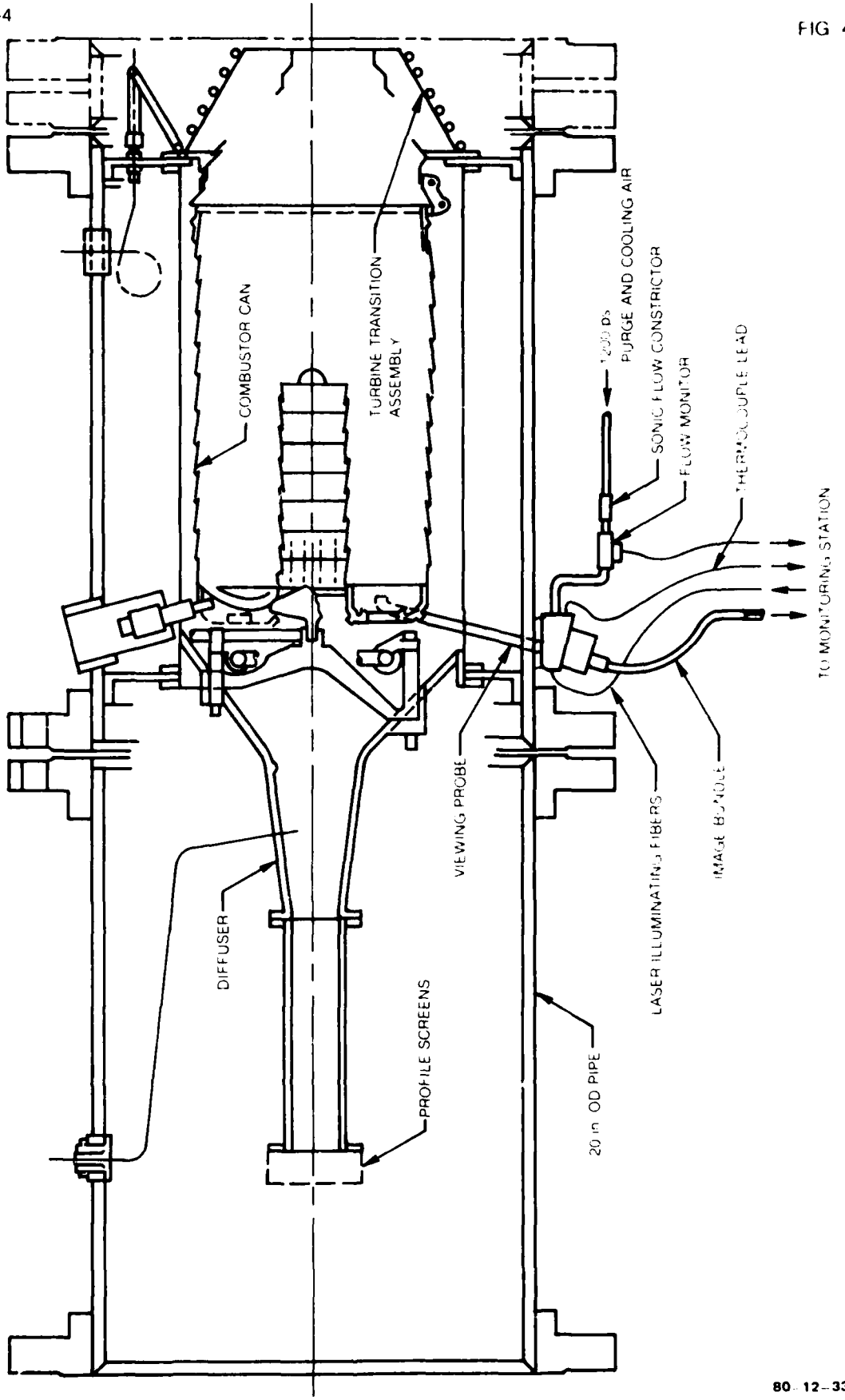

80-12-33-8

FIG 4 3

FT4 TEST SECTION END VIEW

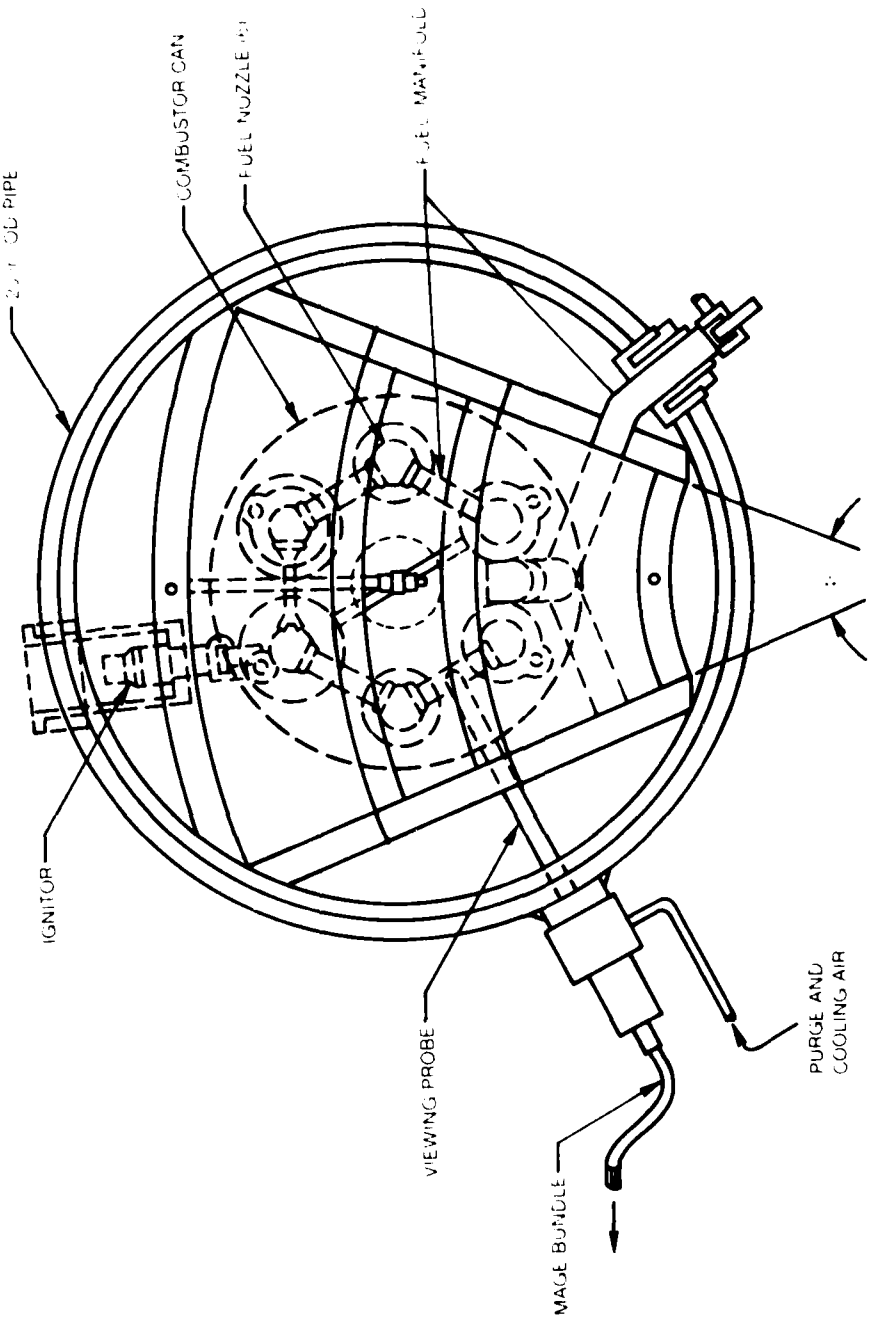

80-12-33-7

on the rig, through the 18 inch burner stand wall, and into a trailer placed adjacent to the outside stand wall. The trailer acted as a monitoring station to use various cameras and instruments with the fiberscope output directly rather than through an elaborate set of remote controls.

4.2 Fiberscope Placement on Rig. The position of the fiberscope on the rig is shown in the side view of Figure 4.2 and in the end view at the combustor inlet of Figure 4.3. The probe mounts to a boss on the outside of the 20 inch diameter rig pipe, passes through a hole placed in the segmenting wall, and then under the fuel manifold lines at a location between two fuel nozzles as shown in the figures. The probe was designed with an 8° angle, tilting forward, from the pipe radius so that we could easily place the probe between the fuel manifold and liner and inset the viewing tip into a half inch hole in the liner that was specially drilled for the probe. The probe could be removed and reinserted from the boss without the time consuming procedure of disassembling the burner rig.

The 1200 psi probe purge and cooling gas line shown in Figure 4.2 along with the sonic flow constrictor, flow monitor, valves, and monitoring gauges that were placed in the trailer. A small water line (not shown in the figures) supplied cooling for the probe mounting head. The laser illuminating fibers and thermocouple leads used the same sealed access port on the probe mounting piece and were not used simultaneously on the fiberscope.

A photograph of the backside or input end of the burner can with the viewing probe installed is shown in Figure 4.4. The diffuser section and fuel manifold were removed so that the position of the probe on the can could be seen. The backside of the half inch diameter probe can be seen protruding through the segmenting wall on the left hand side of the rig in the photograph. The probe tip is inserted into a half inch hole between two fuel nozzle ports and is viewing downstream and parallel to the combustor rig axis.

The view into the can from the opposite direction is shown in Figure 4.5. In this photograph, we can see the tip of the probe protruding slightly into the can at a crease that runs between the fuel nozzle ports. The swirler vanes on the end of the 11 inch long, 3 inch diameter center air tube can also be seen in the photograph.

A photograph of the view of the inside of the burner liner looking through the fiberscope is shown in Figure 4.6. The burner liner center tube can be seen in the righthand side. The picture in Figure 4.6 was taken with the liner outside the rig. A spotlight was moved around the exterior of the liner during the time exposure used for the photograph. As a consequence, several of the dilution holes in the liner appear brightly illuminated. A small sign with inch and a half letters "FT-4" can be seen at the end of the liner in Figure 4.6.

BACK SIDE OF BURNER CAN WITH VIEWING PROBE INSTALLED

81-3-3-2

UPSTREAM VIEW INTO BURNER CAN

FIBERSCOPE VIEW INSIDE FT-4 BURNER CAN

80-12-33-1

4.3 Probe Operation on Rig

4.3.1 Sooting and Temperature Measurements. The region of the combustor liner where the probe tip intrudes has by far the highest levels of carbon soot and coking deposits. This can be seen in Figure 4.5. When the probe was removed and inspected after the first couple of runs, a thin soot deposit had collected in the viewing lens. This soot deposit was not immediately noticed at the output end of the probe, but undoubtedly reduced the light intensity transmitted by the probe a significant amount. The nitrogen exiting the holes around the viewing lens was not in itself sufficient to prevent soot deposition on the outside surface of the viewing lens. This problem was resolved by blocking two of the ten exhaust holes around the viewing lens with small screws. The blocked holes were in opposite sides of the lens. Small channels were then machined in the viewing lens holder to connect the blocked holes with the lens thereby directing a fraction of the cooling gas flow onto the outside surface of the lens. After the modification, the lens remained free of soot. This result is shown in Figure 4.7 which is an enlarged photograph of the probe after 20 minutes of operation in the combustor. One can note the heavy soot deposit on the probe face in the presence of the specular reflection of light from the clean viewing lens at the center of the probe face. The end of the small 10 mil diameter laser illuminating fiber can be seen in the smaller hole at about 2 o'clock in the probe face.

A thermocouple (TC) was placed inside the probe for the first few runs. The TC was first placed into one of the cooling holes that surround the viewing lens to measure the probe tip temperature. Temperatures at this location ranged from 165 to 178°C for full power operation and 120-130°C for half power operation. From the cooling calculations of Section 3.3, we would expect an exit gas temperature of about 108°C for the high power run and 90°C for the low power run. Additional heating of the TC was probably given through lead wire conduction to the much higher surrounding metal surface temperatures.

The TC was also placed on the inside surface of the probe at the point closest to the viewing lens where the image conduit contacts the surface. This location measured the maximum temperature that would be felt by the conduit glass. The temperature at this location, which could not be easily calculated, ranged up to 300°C at full power and to 191°C at half power. These temperatures are well below the 540°C limit of the glass.

4.3.2 35 mm Photographs. During several runs with the viewing probe in the combustor, photographs of the combustor view were taken with a Nikon single lens reflex camera. Ektachrome 35 mm film was used, and during development the film was pushed one stop to give an effective film speed of 800 ASA. The standard Nikon 50 mm, f1.4 camera lens at full aperture with a bellows extension was used to reimage the combustor view from the output end of the fiber bundle

FIG 4 7

END OF VIEWING PROBE AFTER 20 min OF OPERATION IN COMBUSTOR

81-3-3-1

onto the film. Magnification of the 3 mm bundle image from 1.3 to 1.9 was used in taking the pictures. These magnifications do not fill the entire 35 mm camera frame with the combustor view, of course, but we were primarily interested in obtaining maximum light intensity without degrading the resolution of the image. The resolution of the combusotr view at the output end of the film bundle is about 50 ℓ/mm. The resolution of the film is between 80 to 100 ℓ/mm so that the small magnification of the combustor view helped insure that the film did not contribute significanly to image degradation but would allow the shortest possible exposure.

During the first run exposures from 1 to 1/2000 sec were taken. Proper exposure times were determined to be at the 1/1000 to 1/2000 sec shutter speeds. The fast shutter speeds are required in order to "stop" the motion of flame which is rapidly moving in the turbulent combustor. Each exposure shows a different flame pattern which indicates the great variability in the position of the luminous flame during operation of the combustor.

Exposures were taken with blue, greem and red Kodak filters. The blue filters reduced the light levels so significantly that only a weak image could be recorded at 1/60 sec exposure. The flame structure could be observed with the green filter as with no filter and the exposure times were only increased a couple stops. With the red filter, however, a good deal of the flame structure was removed. This result is not completely understood at the present time.

Figure 4.8 shows an enlargement from a 35 mm color slide of the combustor view through the fiberscope. The image quality was reduced somewhat from the original 35 mm color slide. More importantly, the black and white exposure eliminated the brightness contrast and some detail that one can observe in the color transparency. The exposure time for Figure 4.7 was 1/1000 sec. In the figure, one can see the luminous flame burning under the center tube in the combustor can (cf. Figure 4.6). This is only a temporary situation as the position and extent of the burning zone is rapidly changing. The black mark in the view at about "3:30" is a particle of dirt somewhere in the optical system.

The reflection of light from the burner liner surfaces is diffuse, and only a few percent of the incident light from the flame is reflected into the fiberscope view. Since the range of contrasts that can be seen on fiber is about 20:1, the liner surfaces and center tube appear only as shadows or dark zones in the photographs that were taken. In order to view the liner surfaces, using the flame luminosity, one would have to block the direct light from the flame and increase the film exposure 4 to 5 stops to pick up the reflected light.

FIG. 4.8

VIEW OF COMBUSTOR FLAME, EXPOSURE 1/1000 SEC

81-3-3-6

4.3.3 High Speed Motion Pictures. Five rolls of 16 mm Ektachrome high speed tungsten movie film with 100 ft per roll were taken of the combustor view with a Locam camera. Framing rates from 100 to maximum 500 frames per sec were used. There was enough light intensity from the combustor view to make a good exposure at 500 fr/sec. Movies were taken of ignition, burn out, high power and low power operation. When observing the motion pictures with a stop action projector, one can see that even at 500 fr/sec each frame has a different flame pattern that cannot be related to the previous frame. 500 fr/sec is simply not fast enough to follow the flame dynamics. On some frames, for instance, the luminous flame covers only a very small portion of the view as though it were nearly "blown out"; and on other frames almost the entire view is covered by the luminous flame.

In order to take motion pictures at a faster framing rate a greater intensity of light from the combustor view must be made available. A minor modification of the probe was undertaken in which we replaced the original image conduit and transfer lens with a slightly longer conduit rod and support piece to give a pressure seal around the conduit rod. The 9 ft image bundle was butt coupled with a small amount of optical coupling grease to the end of the image conduit. The utilization of butt coupling in place of a transfer lens between the imaging fiber optic components gave about a 5 times enhancement to the light intensity. A carefully constructed pressure seal was required, however, to keep the conduit from moving under the operating pressures of the combustor.

With the butt coupling modification, we were able to take motion pictures at higher framing rates with a Hicam camera. Six rolls of film were taken with framing rates of 1500, 2500, and 5000 fr/sec. There was enough exposure for the 5000 fr/sec rate, and at this rate the flame dynamics could be followed to a reasonable extent. Pieces of flame breaking away and traveling down the combustor could be seen as well as the motion of the flame around the center tube of the liner.

Fuel burning from four nozzles could be observed in the movies from the fiberscope view (cf. Figure 4.4). The flame from the two nozzles adjacent to the viewing probe at times completely filled the probe view. The flame was highly turbulent, however, and frequently would clear to some extent to allow a fiew of the center tube and the flames from the next two adjacent nozzles. The flame from the second nozzle above the probe entrance was particularly noticeable and its motion could be observed along the combustor can.

During an ignition sequence, taken at 500 frames/sec, only three frames (less than 4 msec) was required for the flame to fill the liner. At shutdown, however, when the fuel was turned off, the flame decreased slightly in intensity for about 120 msec and then quickly went out in about 28 msec

(14 frames). A flicker of light from differnet places in the burner can would reappear several times later for about 300 msec after the flame went out.

In general, the high turbulence and changes in the flame pattern appeared to be random. The flame would repeatedly, but not with a constant period, open and close, dim and brighten, fill the entire view and in a rare instance, nearly burn out. These effects were most noticeable when the rig was operated in the 10 MW mode. At 20 MW, or full power, the flame filled the entire view most of the time and burned more intensely from the two adjacent fuel nozzles. There were instances observed at 250 frames/sec where the flame appeared to bounce back and forth. This action may be related to the 270 Hz fluctuation frequency to be discussed later.

The eleven 100 ft rolls of film were reviewed and an edited film of about 300 ft was constructed from various segments of the eleven rolls.

4.3.4 Video Tapes. A Singer GPL 990 vidicon camera with an ir filter and a Sony AV-3650 recorder were used to make a video tape of the combustor view through the fiberscope. The filter was a Rolyn 65.1395 that had a cutoff wavelength near 770 nm to block the visible wavelengths. The long wavelength cutoff at 1000 nm was determined by the vidicon tube response.

A vidicon camera produces an image by making two interlacing scans of 525 lines within a time frame of 30 msec. From the results with the still and movie camera we found that this rate of forming an image is not fast enough to catch the flame pattern and only a smeared image or averaging of flame patterns can be observed, We also found that the contrast with the video camera was poor as compared to the color photography. The poor contrast may have come from the fact that we could not as easily distinguish the high temperature burning zones from the lower temperature zones at the ir wavelengths as in the case when we used red filters with the color photography. We could observe some average brighter zones of burning in the combustor with the video pictures, but the detail was just not as clear as with the color photography and, of course, you could not follow any of the rapidly developing flame dynamics that you could with the high speed color motion pictures.

4.3.5 Emission Spectra. The visible radiation from the combustor comes almost entirely from thermal radiation emitted by hot carbon particles (Ref. 4). These particles are generated in large numbers during the combustion of oil droplets and range in size from 5 nm to 250 nm, which, on the average, is significantly smaller than the wavelength of visible light. The mechanism for the generation of carbon (or soot) particles in oil droplet burning flames is not completely understood and is the subject of many current investigations (Ref. 4, Chap. 8). It is generally accepted that the temperature of the radiating soot particles in the flame closely approaches the temperature of the flame gases. Gaydon and Wolfhard (Ref. 4, Chap. 9) indicate

that there has been substantial agreement on the color temperature of soot particles with the gas temperature in benzene and acetylene flames; and early estimates indicate that the difference in temperature between particle and flame gases caused by radiation losses was on the order of a degree C.

The stable products of combustion (H_2O, CO_2, CO, O_2 and N_2) have no electronic transitions that allow banded emission and absorption spectra in the visible. Some of the unstable molecules (radicals), however, such as CH, C_2, CN, have weak banded spectra in the violet, blue and green wavelength regions. Emission from the unstable molecules is noticeable in clear premixed flames along with a weak continuous radiation from chemical reactions and recombination of ions. The radical OH has a strong emission band at 306.4 nm in the near uv. Berretta, et al. (Ref. 8), have measured the OH emission along the axis of an atmospheric oil burner. They also observed the visible wavelength emissions from C_2 and CH in the clear portion of their flame near the burner nozzle. The emission intensity from C_2 and CH decreased into the noise in the heavy soot generating part of the flame.

In the infrared spectrum from 2 μm to longer wavelengths, the combustion products H_2O, CO_2 and CO emit and absorb strongly at their vibrational transition bands and contribute significantly to the overall emission at these wavelenghts as shown by Claus (Ref. 9). The fiberscope only transmits to wavelengths as long as 1.6 μm, however, and cannot pass the infrared band emissions. The OH radiation at 306 nm is also blocked by the fiberscope. Use of low loss quartz communication fibers would allow transmission of the OH radiation. Image transmitting fiber bundles are not made with the quartz fibers, however, and only nonimaging experiments could be performed with these fibers as optical receivers.

Wavelength spectra were taken of the combustor flame through the fiberscope with a 1/4 meter Jarrell Ash scanning monochromator and an EG&G-PAR optical multichannel analyzer (OMA2) system. The monochromator, which took several minutes to make a scan, plotted the spectra from the visible through the near ir (400 nm to 1150 nm). The OMA2 system, which could make a scan in 20 msec, was set to monitor the emission from 240 nm to 600 nm. An advantage of the OMA2 system, besides making rapid scans, is its ability to make rapid computations with other spectra for comparison. In this case, for instance, we also recorded the spectra from a standard tungsten ribbon lamp at different temperatures through the same fiberscope.

Figure 4.9 shows a trace of the spectra of the combustor flame taken with the OMA2 system. One curve in Figure 4.9 was taken with the combustor at full power and the other at half power. An interesting result of this spectra and also the spectra taken with the scanning monochromator is that the ratio of the spectra at full and half power decreases to about one at the shorter wavelengths. This result will be discussed in Section 5.1.

FIG. 4.9

RADIATION FROM COMBUSTOR THROUGH FIBER OPTIC VIEWING PROBE

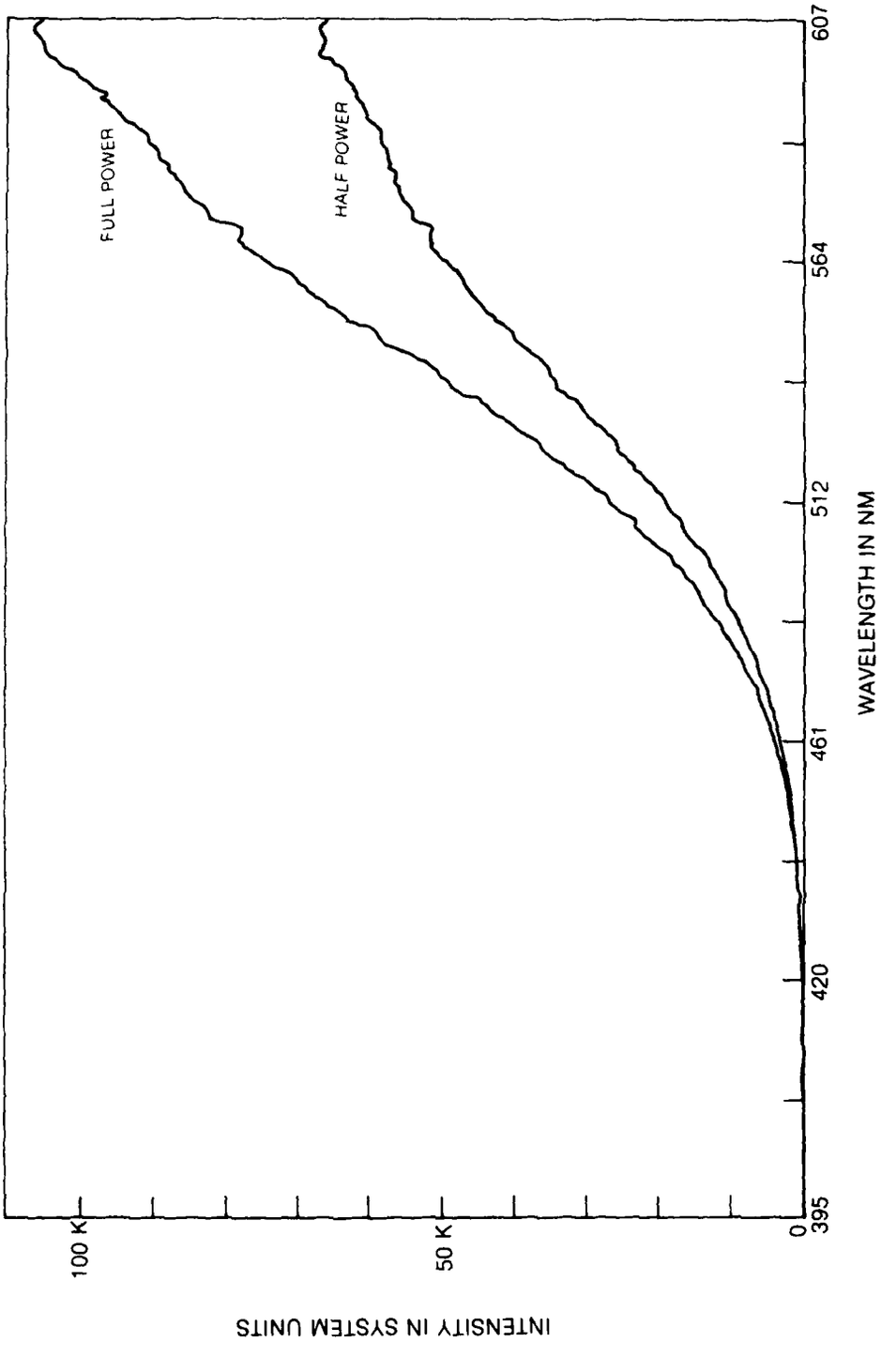

81-6-155-11

The spectra full power was also ratioed with the spectra from a standard tungsten ribber lamp at eight different temperatures from 1300°C to 2100°C. The temperature of the lamp was measured with an optical pyrometer. A plot of the spectral ratios is shown in Figure 4.10. For this figure the ratioed spectra were normalized to 1 at λ 512 nm to allow an easy comparison. It will be shown in Section 5.2 that when the temperatures of the two spectra are equal the spectra ratio is a constant. This result requires that the emissivity be a constant over the range of wavelengths being compared. The spectra for Figures 4.9 and 4.10 were taken over a complete cross section of the burner view and represents a space and time average of the combustor emission. The OMA system was set for 100 scans with 30 msec/scan or a 3 sec time average. The ratioed spectra stay nearly constant in the wavelength range between 540 nm and 607 nm at a lamp temperature between 1540°C and 1600°C. A correction of 133°C has to be added to the lamp temperature to allow for emissivity of the tungsten ribbon and window loss. The indicated average combustor temperature was then about 1700°C.

One could, in principle, sample smaller sections of the burner view and measure hot zone temperatures. Using fast time gating with the OMA vidicon tube, the temperature of shorter lived burning regions could also be measured if enough light intensity is available from the burning region.

The small structure that appears in the spectra of Figures 4.9 and 4.10 at 570 nm and 600 nm is not understood at the present time and may be an instrumental or noise error.

4.3.6 Fluctuation Spectra. An enclosed combustion chamber will have characteristic acoustic frequencies which are determined by its dimensions and the velocity of sound through the burning gases. Acoustic vibrations may couple with or be driven by the varying heat release rate of a burning flame (Ref. 4, Chap. 7). Such periodic vibrations in large combustion systems are undesirable and may be dangerous due to possible loss of flame stability and destruction of metal parts, including fatigue failure of metals.

We measured the flame motion in the combustor by positioning with a 3-D micropositioner a cut and polished end of a single fiber at the output of the 9 ft image bundle. With this system we could pick-up the optical signal from any 0.2 mm dia segment of the 3 mm dia combustor view. A photodetector was placed at the other end of the optical fiber pick-up, and the detected signal was amplified by a Tektronics 1A7A amplifier that had an adjustable bandwidth. The amplified signal was then sent to a Spectral Dynamics SD340 Fast Fourier Transform (FFT) Analyzer. With this instrument, we could measure the spectra of the flame fluctuations from different segments of the combustor view. The spectra were generated in 20 msec; and 8, 16, 32, and 64 scan averages could be taken. A typical power spectrum of the flame fluctuations

RATIO OF SPECTRUM FROM STANDARD LAMP TO SPECTRUM FROM COMBUSTOR VIEW

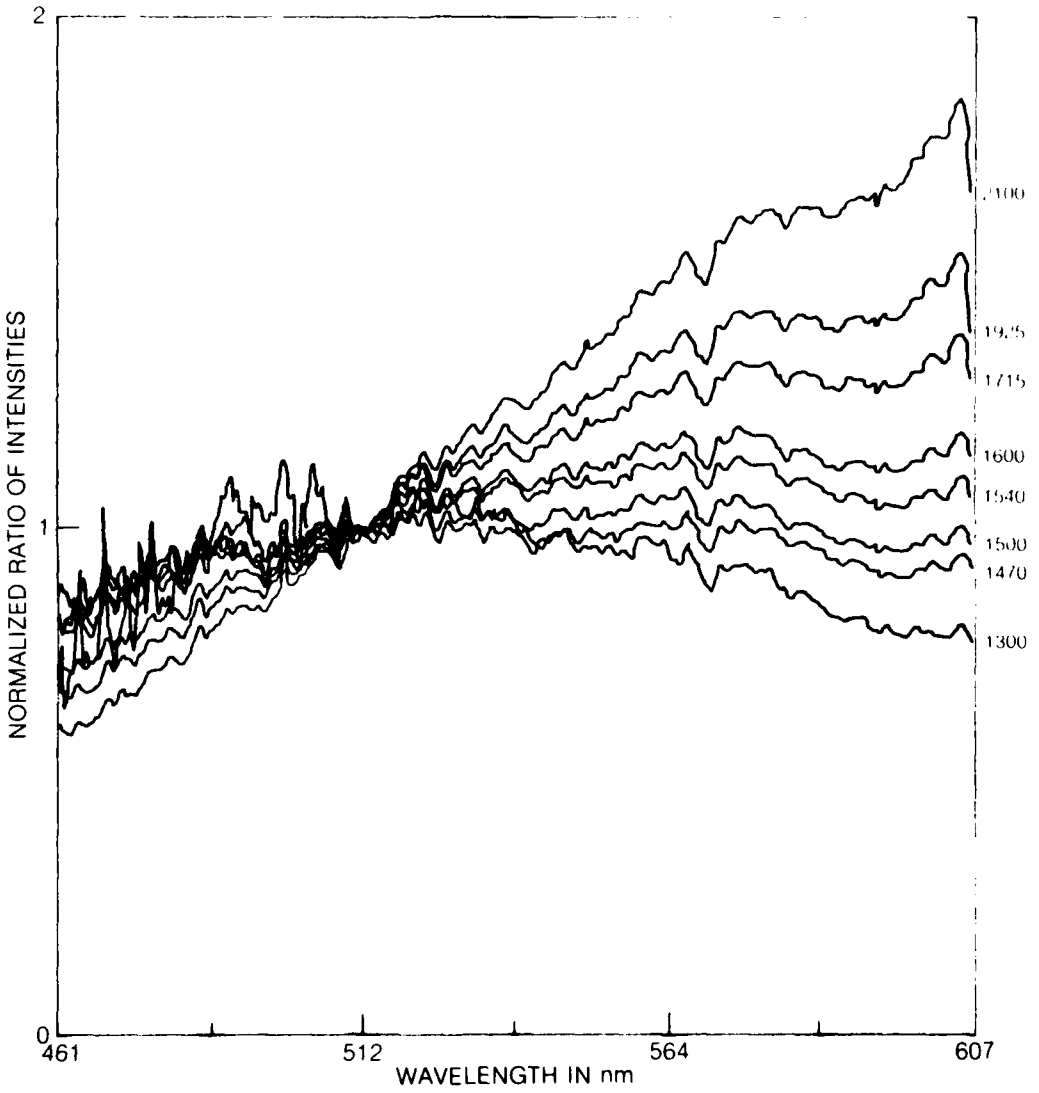

81-3-3-3

is shown in Figure 4.11. Most of the spectra is generated by random turbulence of the burning flame. Observing the spectra in real-time, we could follow the rise and fall of short lived resonances at certain frequencies in the burner spectra. The most prominant peak occurred at about 270 Hz as indicated in Figure 4.11. Resonant frequencies for acoustic modes that travel around the burner can annulus would be in the range of several kHz at the average combustor temperature. The 270 Hz signal observed with the FFT Analyzer may arise from an axial mode that occurs from a reflection about 1 meter down the length of the rig from the combustor inlet where the rig tubing makes a reduction in diameter. This distance and frequency agrees with an average sound velocity in 1000°C air.

By releasing heat in local zones and at varying rates, the flame motion will in part drive and be driven by the turbulence of the flowing gas and by acoustic resonances that may occur in the combustor. This coupling may be important for flame stability and mechanical integrity of the engine parts. An unstable or an acoustically modified flame, for instance, could generate undesirable temperature pattern factors at the turbine inlet under certain engine operating conditions.

4.3.7 Laser Illumination. Two 15 ft lengths of single optical fiber were used to transport an argon laser beam through the fiberscope for an illumination source. The fibers terminated at the end of two smaller holes on the cooling hole circle surrounding the viewing lens (cf. Figure 2.4). One fiber, Galite 3000 LC, had a 200 μm core dia and was coarse ground on the output end to scatter the illuminating light in a 180° wide angle. The second fiber was a 63 μm core Corning fiber that had a low numerical aperture of 0.14 giving a spread of 16° to the illuminating laser beam.

The illumination patterns from the multimode fibers with coherent laser light are not continuous but broken into many patches of various sizes due to interference between the different modes of the fiber. This type of illumination that also produces speckle may not be the best for examination of surfaces, for instance, but may be acceptable to examine fuel spray patterns. In contrast to an incoherent light source, which would require a bundle of fibers for transmission of sufficient light, the entire laser source can be focused into and transported by a single fiber.

The wide angle illuminating fiber broke during a lens adjustment, but the narrow angle emitting fiber survived and can be seen protruding slightly from its hole at "2 o'clock" on the probe tip in Figure 4.7.

During a combustor run, a 3 watt argon ion laser beam was focused into the narrow angle fiber. The reflection of the emerging beam from vapors in the burner could be seen when the rig was not operating. When the high velocity air to the rig was initiated the vapors were blown away and only an occasional

FIG. 4.11

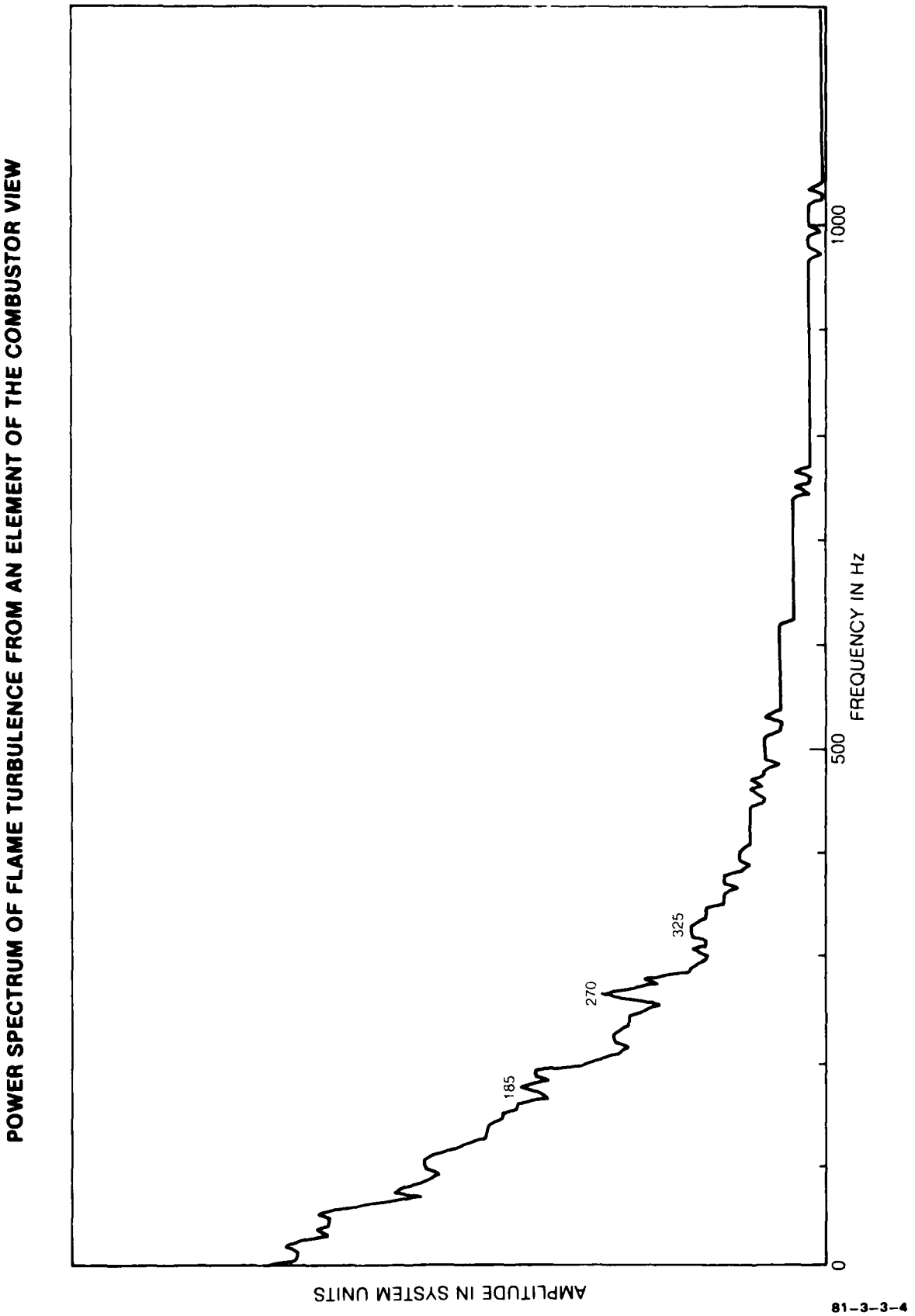
POWER SPECTRUM OF FLAME TURBULENCE FROM AN ELEMENT OF THE COMBUSTOR VIEW
AMPLITUDE IN SYSTEM UNITS
0
500
1000
FREQUENCY IN Hz
185
270
325
81-3-3-4

scintillation from a particle passing through the laser beam could be observed. At the initiation of the fuel spray a bright illumination appeared from the backscatter of the laser beam from the fuel droplets; and after ignition, the laser beam could be seen reflecting from the fuel spray and disappearing into the burning flame zone. Several still camera pictures were taken of the laser illumination in the burner. With the wide angle illumination we could have obtained the entire fuel spray pattern in the field-of-view of the fiberscope.

Laser diagnostics such as laser Doppler velocimetry (LDV), particle sizing, laser induced fluorescence (LIF), Raman scattering, and coherent anti-Stokes Raman scattering (CARS) have been developed for applications to combustion over the last several years (Refs. 10-15). These systems require multiports at different angles for transmitting and receiving apertures, sometimes require large collecting optics, and have been used exclusively in low pressure laboratory flames where unlimited access is available. The fiberscope may be useful in some diagnostic applications to the combustor as a receiving device for scattered laser light that has been injected into the combustion region through two or more additional probes. By actuating the laser probes to different positions, a map of the measured signal could be made over the FOV of the fiberscope. The use of optical fibers and micro lenses for injection of the laser beam into the combustor permits the design of small probes that would be convenient for engines where a limited access exists. Moreover, if only a single position or a small FOV is needed, the fiberscope could be replaced by a much simpler single fiber or small fiber bundle and lens to permit a simplification of the receiver design.

The heavily soot ladened oil droplet burning flames make laser diagnostics more difficult in a real gas turbine combustion, as demonstrated by Eckbreth (Ref. 13), rather than in a premixed, clean burning, nonturbulent laboratory flame. Significant progress has been made recently, however, by Eckbreth with CARS (Ref. 14) measurements and by Beretta, et al. with laser light scattering in emission and extinction spectroscopy (Ref. 15). In addition, LDV systems have been well developed for sometime and are used in many gas dynamic experiments (Ref. 10). The use of fiber optics will allow for easier application of these diagnostic systems to combustors where limited access would otherwise prevent their use. Optical fibers are being used in current CARS system designs at UTRC to receive and transmit the coherent anti-Stokes generated signal to the spectrum analyzing system. The required intensity of the CARS laser input, however, is too great for transmission by optical fibers (> 100 mW/cm^2) and larger discrete optics must be used.

5. ANALYSIS

5.1 Wavelength Spectra. Flame spectra were taken at the two combustion operating conditions of full power (20 MW) and half power (10 MW). As discussed previously, the emission originated from thermal radiation of the combustion generated soot particles. The spectral data was taken over a strip of the entire combustor view corresponding to a magnified monochrotor slit width; and therefore, were a composite of many different temperatures summed from different positions in the burner and over a period of time corresponding to the instrument integration time. Since the burner flame at full power was brighter and filled a greater portion of the burner view more of the time than at half power, one would expect the spectral intensity at full power to be greater than at half power. This was the case, of course, as can be seen in Fig. 4.9. What was unexpected, though, was the fact that the increase in spectral intensity was considerably greater at the longer wavelengths than at the shorter wavelengths. If the emission temperatures of the particulate were the same and the full power operation just had more emitting particles than at half power, then the spectra would increase proportionally at all wavelengths. In fact, though, there is a wide temperature distribution among the particulates; and at full power we should detect a higher average color temperature for the spectral emission. In this case one would expect the spectral intensity at shorter wavelengths to increase more than the longer wavelengths when the combustor operation goes from half to full power. For instance, if we compare the blackbody (or gray body) emission at temperatures of 1700°C and 1500°C at a wavelength of 1.0 μm, the emission ratio would be 2.4. At a shorter wavelength of 0.5 μm this emission ratio would increase to about 4.8.

The change in emission ratios with wavelength can be determined easily for gray body emitters. Planck's radiation equation for the spectral radiance:

$$N_\lambda = \frac{\epsilon\, C_1}{\lambda^5 (e^{C2/\lambda T} - 1)}$$

reduces to Wiens' equation

$$N_\lambda \simeq \epsilon C_1 e^{-C_2/\lambda T}/\lambda^5$$

when $C_2/\lambda T \geq 5$. Under this condition the errors in neglecting the -1 in Planck's equation will be less than a percent. For the temperatures and wavelengths we are dealing with $C_2/\lambda T > 5.5$ and we can use Wien's equation.

Consider the optical power per unit wavelength interval emitted at the two operating conditions, 10 and 20 MW.

$$P_{20} \propto (C_1/\lambda^5)e^{-C_2/\lambda T_{20}}$$

$$P_{10} \propto (C_1/\lambda^5)e^{-C_2/\lambda T_{10}}$$

Their ratio is

$$= K\exp\left[C_2\left(\frac{1}{T_{10}} - \frac{1}{T_{20}}\right)/\lambda\right]$$

$$\gamma = P_{20}/P_{10} = K\, e\left[\frac{C_2}{\lambda}\left(\frac{1}{T_{10}} - \frac{1}{T_{20}}\right)\right]$$

where K is a constant independent of λ and T. Since $T_{20} > T_{10}$, γ will decrease with increasing λ. That is,

$$\frac{d\gamma}{d\lambda} = -\gamma\,\frac{C_2}{\lambda^2}\left(\frac{1}{T_{10}} - \frac{1}{T_{20}}\right) < 0.$$

The actual ratio of spectra at the two power levels, shown in Fig. 5.1, behaves just the opposite than expected from the discussion above, and increases with increasing wavelength. A possible cause for the increase in the ratio of spectra at 10 and 20 MW is a wavelength dependent absorption and scattering of the radiation by intervening cooler soot particles and/or fuel spray dropletts. The soot particles are considerably smaller than the observed wavelengths and would scatter in proportion to λ^{-4} (Rayleigh's law). The larger fuel spray droplets would scatter according to Mie theory. For the larger unburned fuel droplets in the 10 μm to 100 μm size the Mie scattering would be strongest in the forward direction, have a total extinction equal to about twice the geometrical droplet cross sectional area, and be relatively independent of wavelength. For smaller droplets or larger droplets that have vaporized to a smaller size than about 10 μm, the Mie scattering would become wavelength dependent and scatter more strongly at the shorter wavelengths as described by Foster (Ref. 16). The radiation transmitted to the fiberscope may then be filtered by cooler intervening particulates to significantly reduce the blue wavelengths in relation to the red wavelengths as in a sunset. We can infer then that the operation of the burner rig at full power produces a higher density fuel spray and soot particles which more strongly filters the shorter wavelengths to reduce the increased emission at these wavelengths.

FIG 5.1

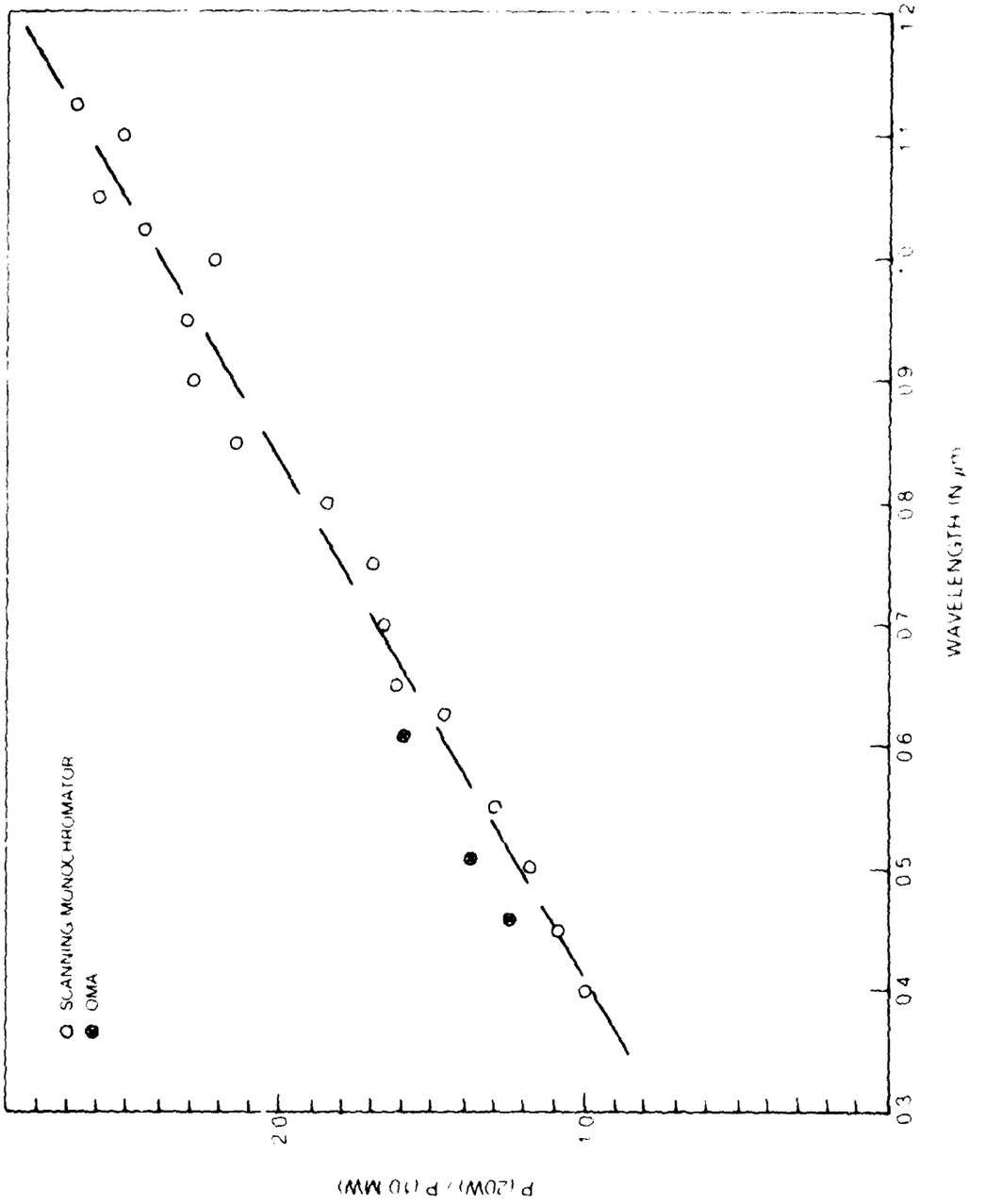
RATIO OF SPECTRA AT 10 AND 20 MW OPERATING CONDITIONS
SCANNING MONOCHROMATOR
OMA
P (20W) / P (10 MW)
WAVELENGTH IN μm
2.0
1.0
0.3
0.4
0.5
0.6
0.7
0.8
0.9
1.0
1.1
1.2
81 6 155 10

If the transmission function through the particulates is given by:

$$\gamma(\lambda) = e^{-k/\lambda^{\alpha}}$$

where k is related to the density of scatters and path length, and $1/\lambda^{\alpha}$ the wavelength dependence, the change in spectra ratio would then be given by:

$$\frac{d\gamma}{d\lambda} = \gamma \left[\frac{\alpha}{\lambda^{\alpha+1}} (k_{20} - k_{10}) - \frac{C_2}{\lambda^2} \left(\frac{1}{T_{10}} - \frac{1}{T_{20}} \right) \right]$$

This result is positive if the scattering term is greater than the temperature dependent term and would therefore produce an increasing ratio with increasing wavelength as observed.

5.2 Flame Temperature Measurement. The derivation of the exact formulation for the emission from a large volume of radiating soot particles would require the solution of the equation of radiative transfer in an emitting, absorbing, and scattering medium. This is a difficult problem. Besides, the exact conditions of the flame, such as particle density, size distribution, and temperature distribution, are not completely known a priori, and these quantities are required for an exact solution. A simplified formulation can be used that requires empirical data in part and can give adequate results to determine a mean temperature of a luminous region of emitting soot particles.

Assume we have a distribution of radiating particles in the field-of-view of the fiberscope with a mean cross sectional area, mean density and mean temperature. Between the radiating particles and fiberscope are much cooler soot particles and fuel droplets that absorb and scatter the radiation on its way to the fiberscope. If the particles emit according to Wein's equation, the radiation incident in the fiberscope would be given by

$$I(\lambda) = K\tau(\lambda)\varepsilon(\lambda)\, C_1 e^{-C_2/\lambda T}/\lambda^5 \qquad (1)$$

where K is a geometrical constant proportional to the field-of-view. The emissivity of the radiating particles is given by

$$\varepsilon(\lambda) = 1-e^{-k/\lambda^n} \tag{2}$$

Various values have been reported for the exponent n in the expression for $\varepsilon(\lambda)$ depending on the type of burner and the location of the radiation from different parts of the flame. Beretta et al. (loc.cit), for instance, measured a value r = 2.25 in the clear sections of their atmospheric oil burner. In the portions of the flame that contained a higher density of soot particles the value of n reduced to a constant 1.5.

$\tau(\lambda)$ in Eq. 1 represents the wavelength dependent transmission function for the radiation passing through the zone of cooler scattering particles that could include recirculating soot particles and vaporizing fuel droplets. This function is represented by

$$\tau(\lambda) = e^{-h/\lambda^a}$$

The radiation from a blackbody source at temperature T_o incident on the fiberscope would be given by

$$I_o(\lambda) = K_o\ C_1\ e^{-C_2/\lambda T_o}/\lambda^5$$

where K_o represents the geometrical constant for the measurement. The ratio of the two spectra is given by

$$\gamma(\lambda) = \frac{K_1}{K_o}\ \tau(\lambda)\ \varepsilon(\lambda)\ e^{-\frac{C_2}{\lambda}\left[\frac{1}{T}-\frac{1}{T_o}\right]} \tag{3}$$

We will examine three cases. In case 1 the region of luminous soot particles is nearly optically dense so that $\varepsilon(\lambda) \approx 1$, and there is no wavelength dependent scattering in the intervening space between the luminosity and viewing system (i.e. τ = constant). In this instance γ increases with wavelength for temperatures $T < T_o$ and decreases with wavelength for $T > T_o$. When $T = T_o$, γ becomes a constant independent of wavelength. In this case the mean temperature of the luminous region would be relatively easily to determine with an OMA system by matching the soot particle spectra with a blackbody spectrum to give a flat γ curve.

The second case, where we have an optically dense medium and a wavelength dependent transmission function, more nearly describes the spectra we observed from behind the fuel spray in the combustor. In this case

$$\gamma = (K/K_o)\, e^{-\frac{C_2}{\lambda}\left(\frac{1}{T}-\frac{1}{T_o}\right)-\frac{h\ell}{\lambda^{\alpha}}} \tag{4}$$

The derrivative or slope of γ is

$$\frac{d\gamma}{d\lambda} = \left[\frac{C_2}{\lambda^2}\left(\frac{1}{T}-\frac{1}{T_o}\right)+\frac{\alpha h\ell}{\lambda^{\alpha+1}}\right]\gamma \tag{5}$$

If $T \leq T_o$ then γ will increase with wavelength. When $T > T_o$, however, the function $\gamma(\lambda)$ can have a maximum at a certain wavelength. That is, the function turns over and decreases in wavelength. We have a maximum when $d\gamma/d\lambda$ is zero. At this condition

$$\frac{1}{T}-\frac{1}{T_o} = -\frac{\alpha h\ell}{C_2\lambda^{\alpha-1}} \tag{6}$$

The second derivative reduces to

$$\frac{d^2\gamma}{d\lambda^2} = -\alpha(\alpha-1)h\ell/\lambda^{\alpha+2} \tag{7}$$

at the zero slope wavelength. This wavelength represents a maximum when the second derivative is less than zero. This condition occurs provided $\alpha > 1$, which is the usual case. Refering to figure 4.9, we see that the spectral ratio turns over at temperature near 1540°C at a wavelength of about 540 μm.

For the third case we will consider the emitting medium to be partially transparent, with $\varepsilon(\lambda)$ given gy Eq. 2, and the transmission function nearly 1 for all wavelengths. This case would describe an observation of the combustor flame from the side of the burner can looking radially inward,

for instance. The spectral ratio is now given by

$$\gamma = (1 - e^{-k/\lambda^n})\, e^{-\frac{C_2}{\lambda}\left(\frac{1}{T} - \frac{1}{T_o}\right)} \tag{8}$$

The derivative of Eq. 8 gives

$$\frac{d\gamma}{d\lambda} = \left[\frac{C_2}{\lambda^2}\left(\frac{1}{T} - \frac{1}{T_o}\right) - \frac{nk}{\lambda^{n+1}} \frac{e^{-k/\lambda^n}}{1 - e^{-k/\lambda^n}} \right] \gamma(\lambda)$$

The derivative is always negative if $T > T_o$ and γ will decrease with wavelength in this case. When $T < T_o$ we have a condition where the slope can go to zero. At the zero slope condition

$$\frac{1}{T} - \frac{1}{T_o} = \frac{nk}{C_2 \lambda^{n-1}} \frac{e^{-k/\lambda^n}}{1-e^{-k/\lambda n}} \; ; \tag{9}$$

and the second derivative which gives the curvature is given by

$$\frac{d^2\gamma}{d\lambda^2} = \left\{ (n-1) - \frac{nk}{\lambda^n}\left[1 - \frac{e^{-k/\lambda^n}}{(1-e^{-k/\lambda n})} \right] \right\} \frac{nk}{\lambda^{n+2}} \frac{e^{-k/\lambda^n}}{(1-e^{-k/\lambda n})} \gamma(\lambda) \tag{10}$$

For an optically thin medium where $k/\lambda^n << 1$ in the wavelength range of interest, the second derivative is greater than zero and a minimum point occurs at some wavelength. This condition is in contrast with case 2 where we had a maximum condition. When the quantity k/λ^n, which determines the degree of optical thickness, is about .7 the second derivative is zero; and for $k/\lambda^n > .7$ the medium becomes more dense and we again have a condition for a maximum instead of a minimum in the spectral ratio.

The use of an optical multichannel analyzer with machine computation would allow curve fitting of Eq. 8 with spectral data ratioed with different blackbody temperatures. We should then be able to determine a mean emission temperature from the luminous soot particles. The mean temperature would be weighted to the higher temperature of the distribution along the view. If we are looking at a hot streak of dense flame the measured temperature would correspond nearly to the peak emission temperature of the flame. On the other hand, if the flame is more dispersed and optically thin the temperature would correspond more nearly to an average along the path.

In cases where we could view a hot surface and the intervening particulate emission was small (very optically thin) we could measure the surface temperature. Care would have to be taken to account for reflected radiation from the hotter flame emission not in the field-of-view as was done by Atkinson and Strange in Ref. 3.

5.3 Contour Plots. A strip containing 12 frames was cut from the high speed motion picture film that was taken at 5000 frames/sec. The film strip was taken to Pratt and Whitney Aircraft's image processing laboratory, and with the use of an Optronics drum scanner and PDP-11/34 minicomputer each frame was digitized in a 64 x 64 array. Both logarithmic and linear density values were recorded for each frame. The data was placed on magnetic tape and then read into the Research Center's Univac computer. A program routine had been previously generated that prints out hard copy contour plots from the digitized data. Figures 5.2 through 5.11 show a sequence of 10 frames from the computer print out. These figures were printed from the linear density data inverted as transmission intensity. Five contour levels were plotted corresponding to levels of 3%, 26%, 50%, 74%, and 97% of peak transmission. A particle, that appeared somewhere in the optical chain, has been darkened to indicate its location in the picutre. In the movies and photographs the particle is quite conspicuous. Since each frame was not perfectly aligned on the drum scanner, the particle was an aid in locating the relative flame position from frame-to-frame. The approximate location of the center tube and end of the burner can (cf. Fig. 4.6) has been indicated on the contour plots in each frame. For illustration purposes, in each of the contour plots the hottest zone (97% transmitting) has been double cross hatched and the second hottest zones (74% transmitting) singly cross hatched.

CONTOUR PLOT FRAME 1

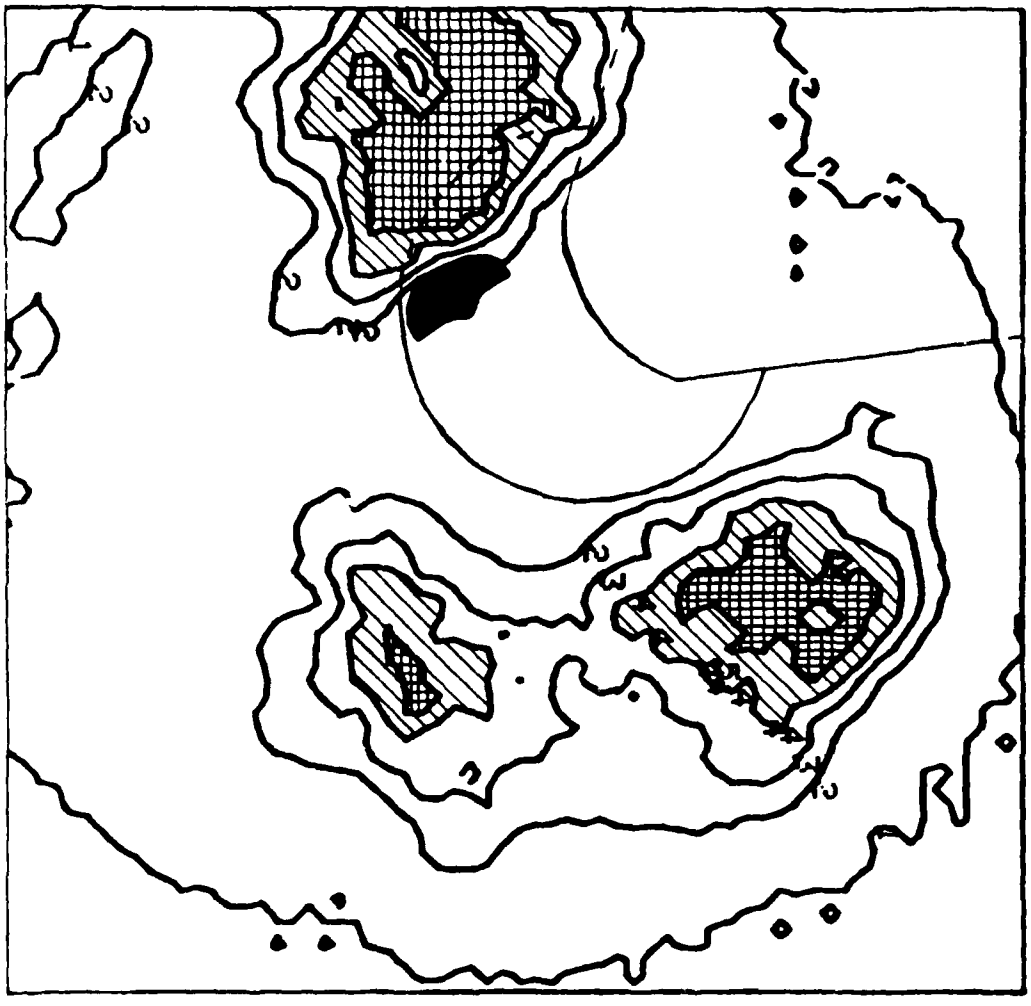

81-6-155-12

CONTOUR PLOT FRAME 2

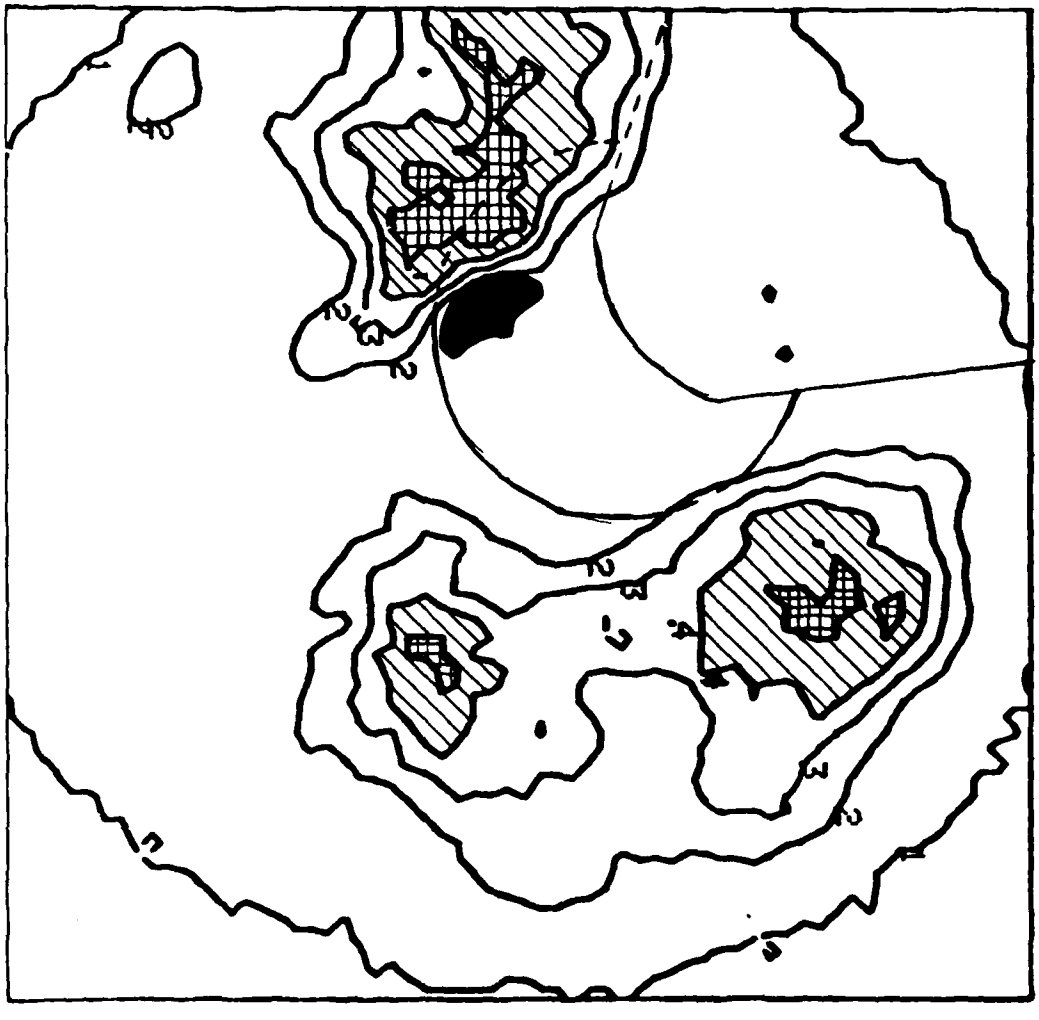

81-6-155-13

CONTOUR PLOT FRAME 3

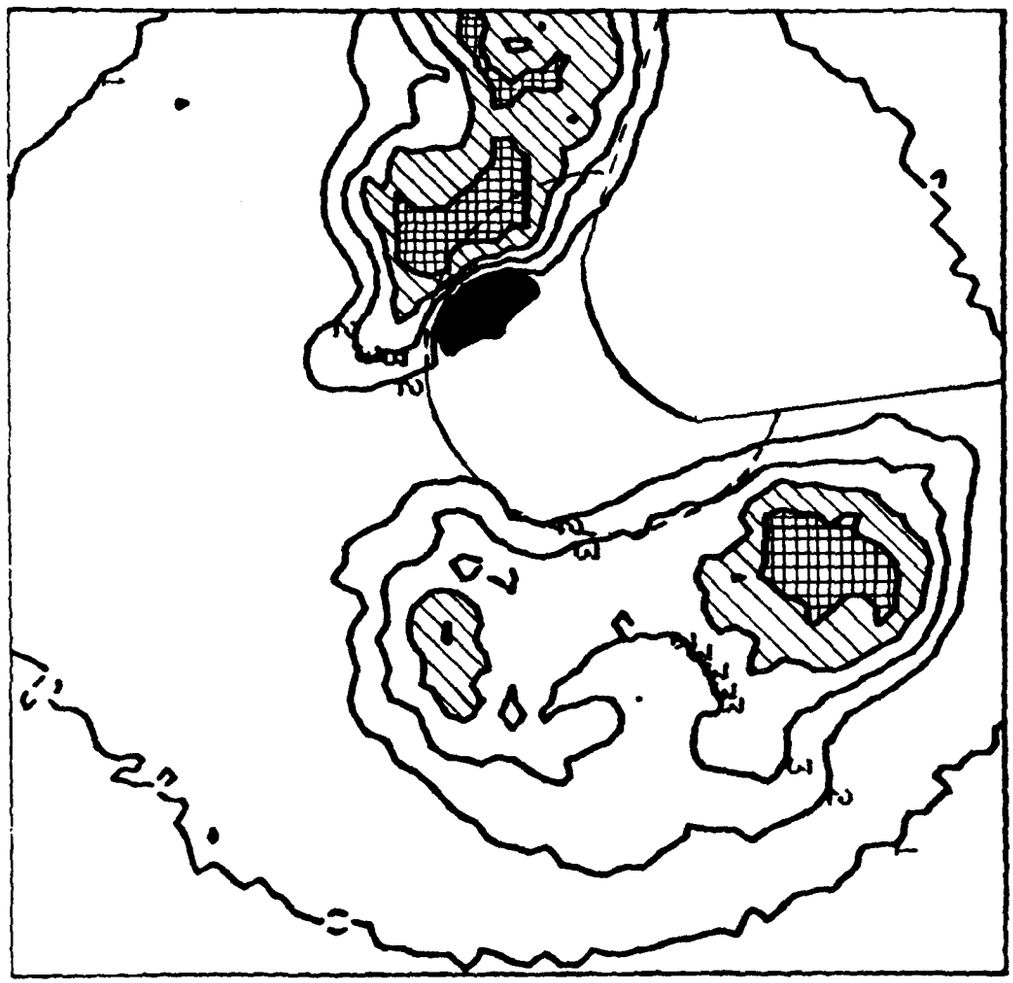

81-6-155--14

FIG. 5.5

CONTOUR PLOT FRAME 4

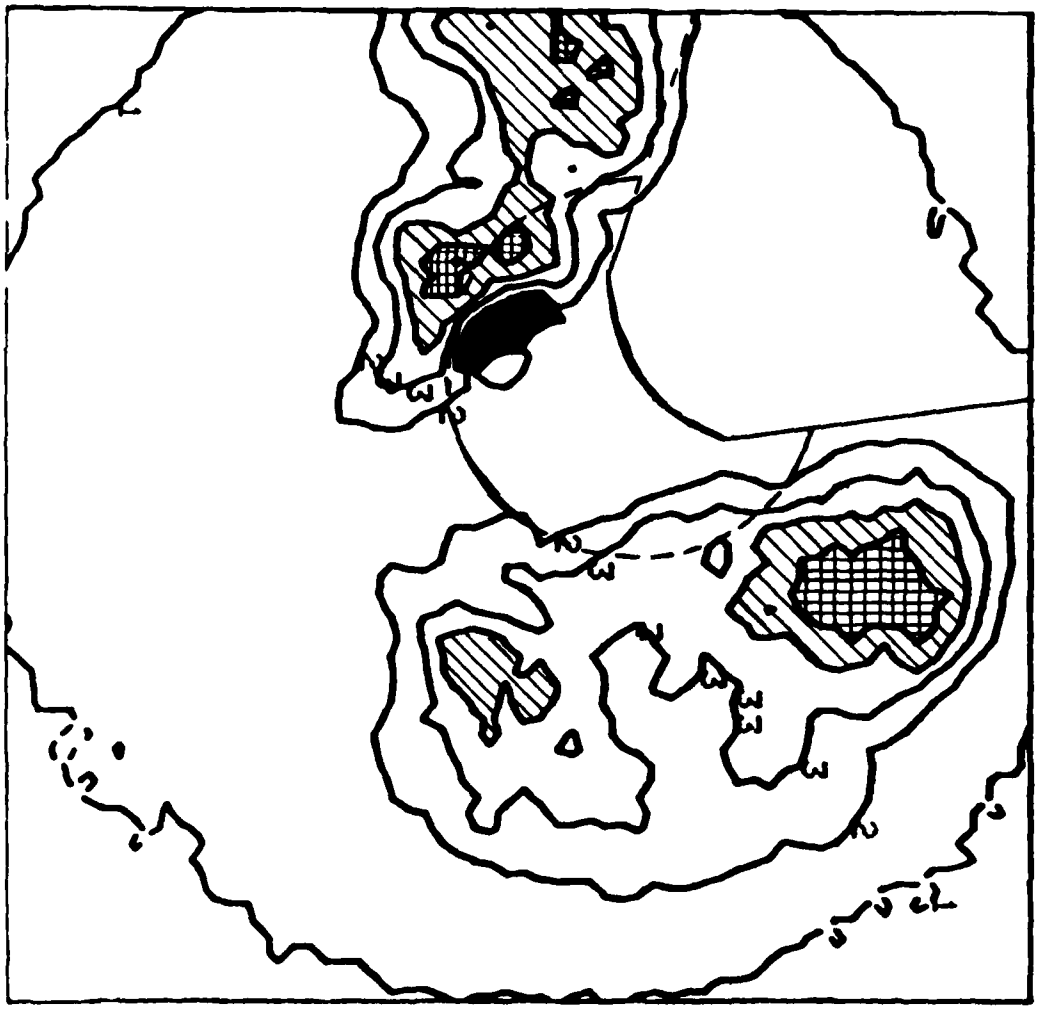

81-6-155-15

CONTOUR PLOT FRAME 5

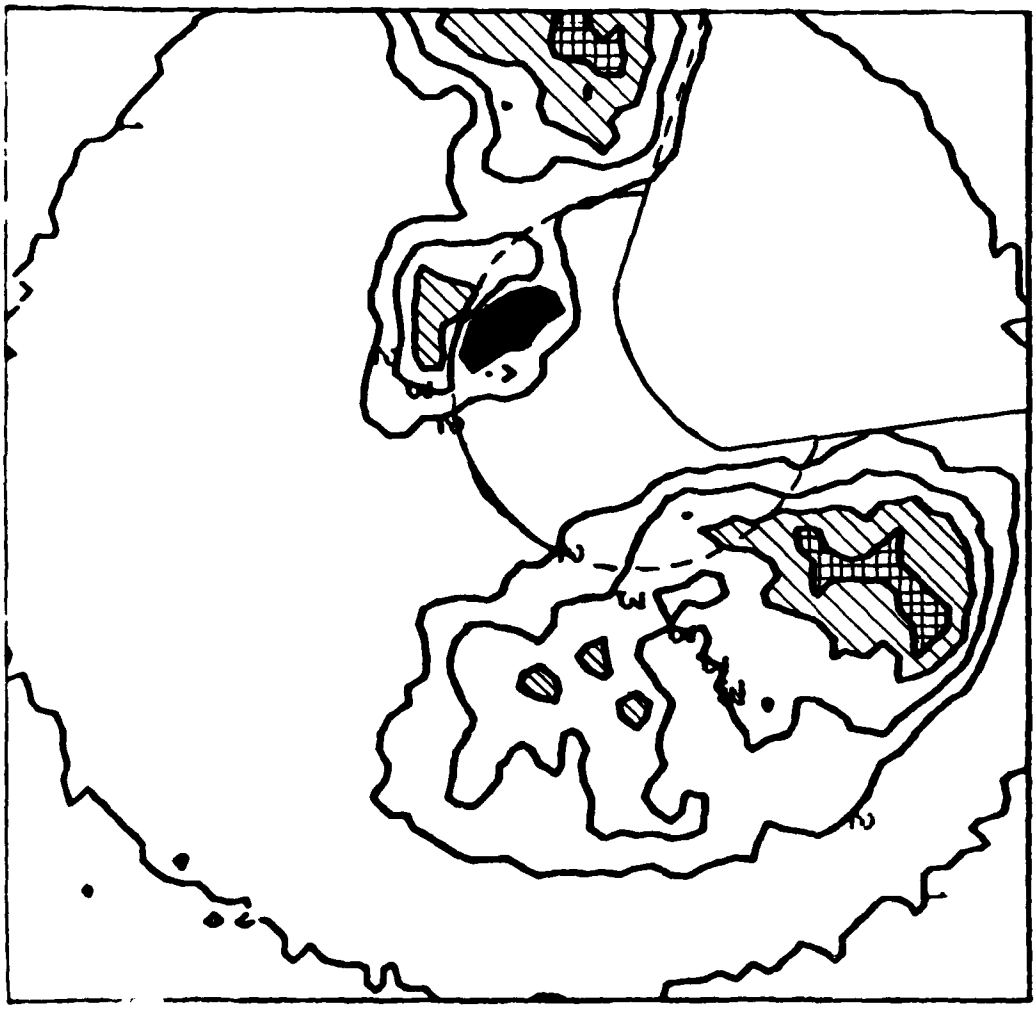

81-6-155-16

CONTOUR PLOT FRAME 6

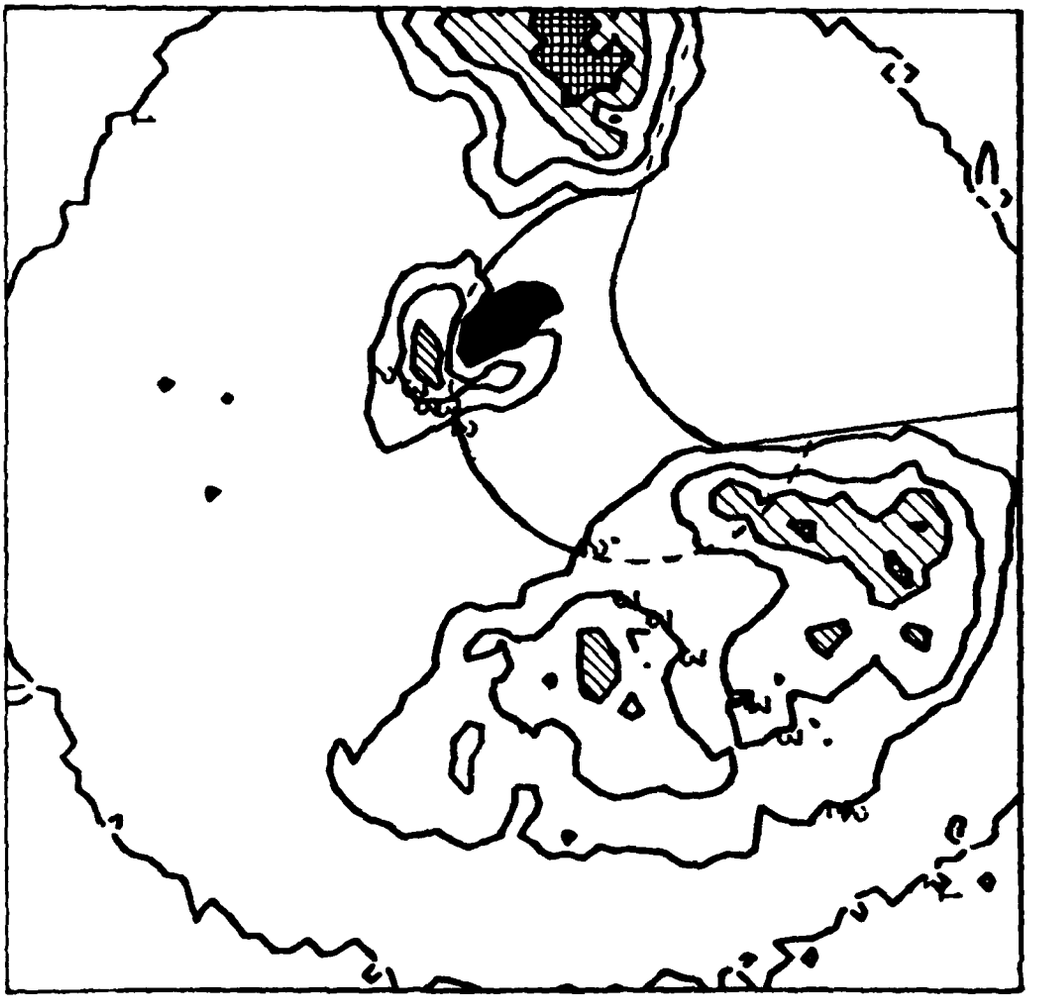

81-6--155-17

CONTOUR PLOT FRAME 7

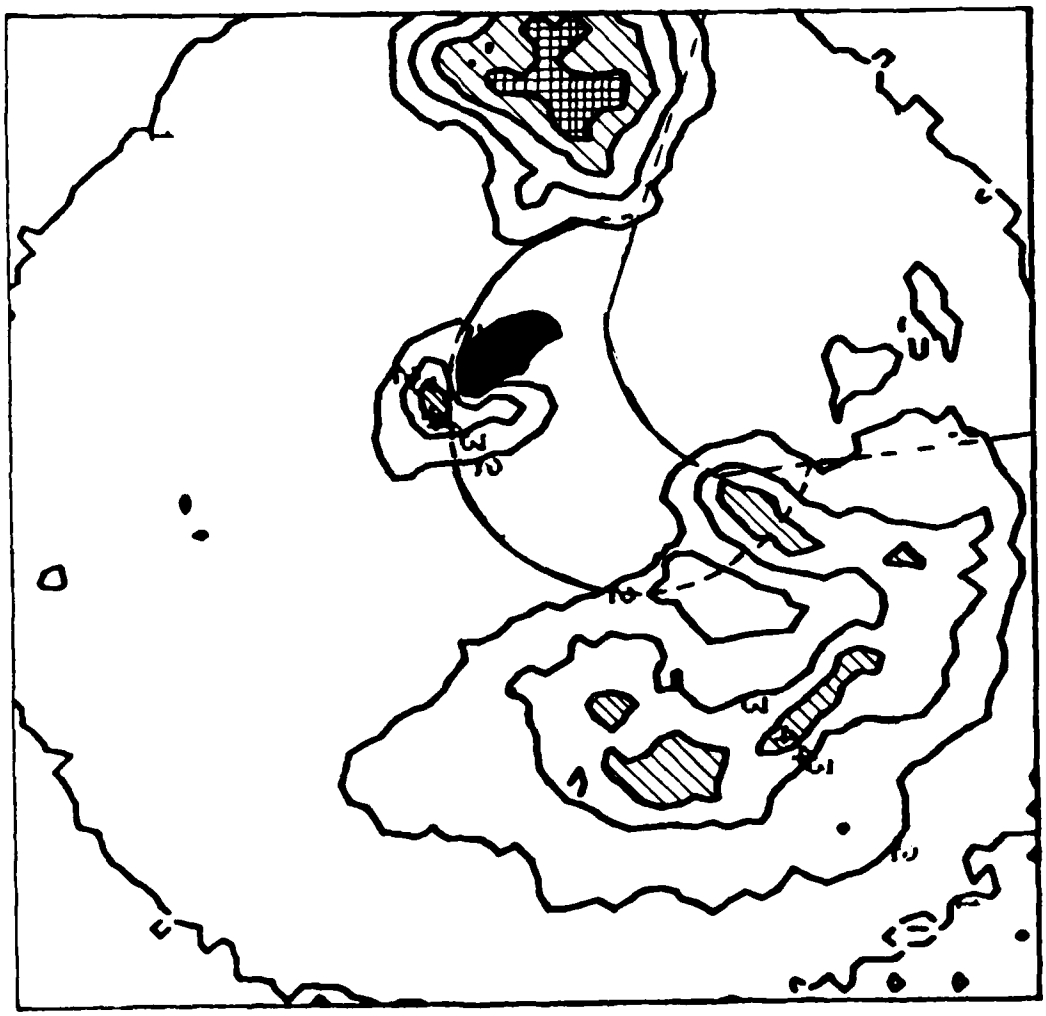

81-6-155-18

CONTOUR PLOT FRAME 8

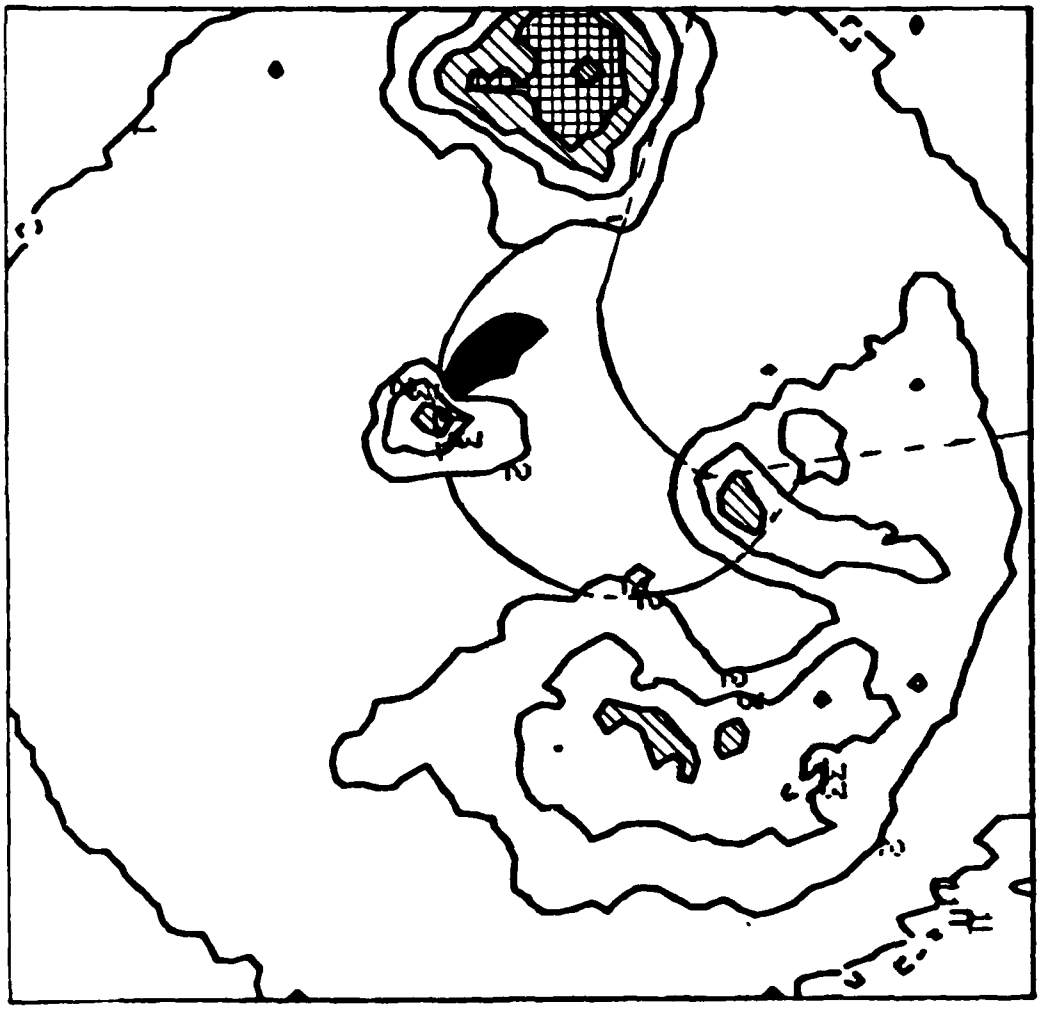

81-6-155-19

CONTOUR PLOT FRAME 9

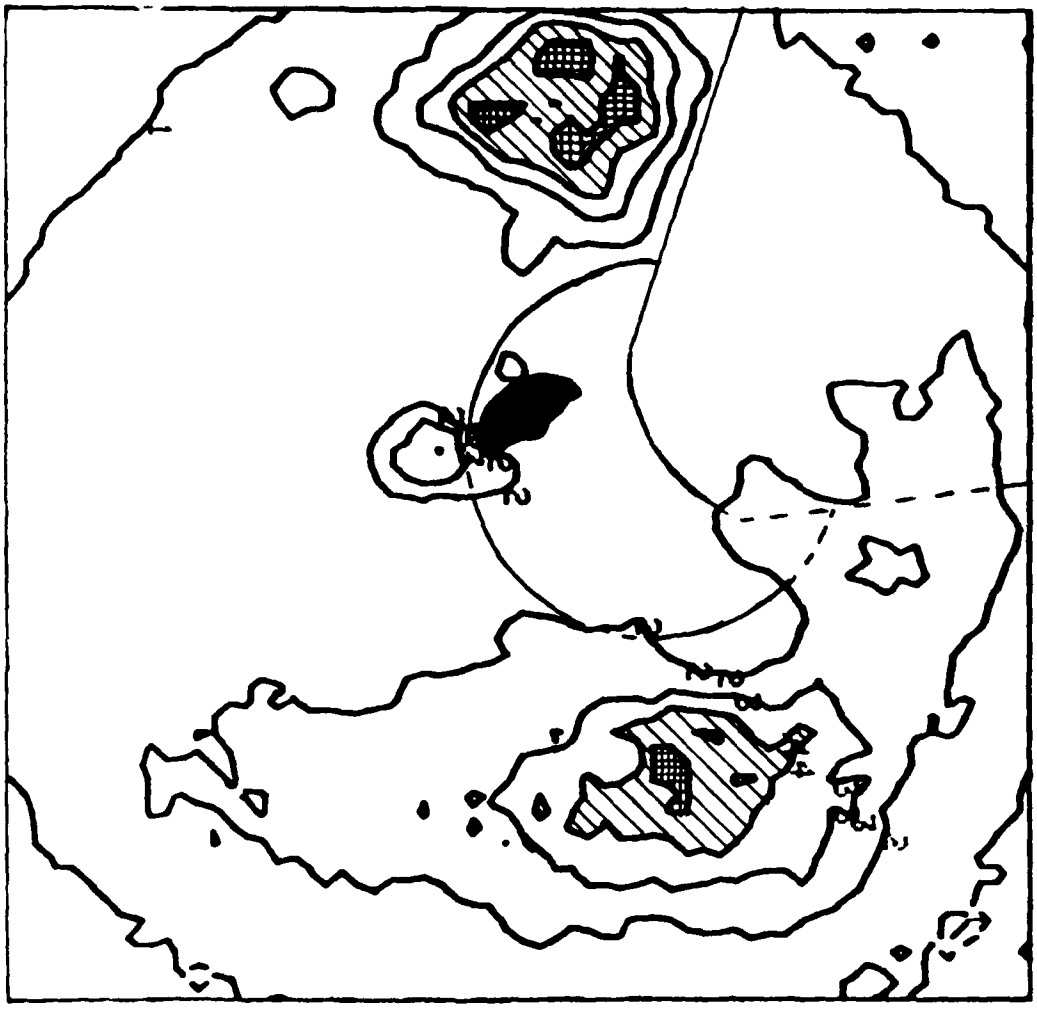

81-6-155-20

CONTOUR PLOT FRAME 10

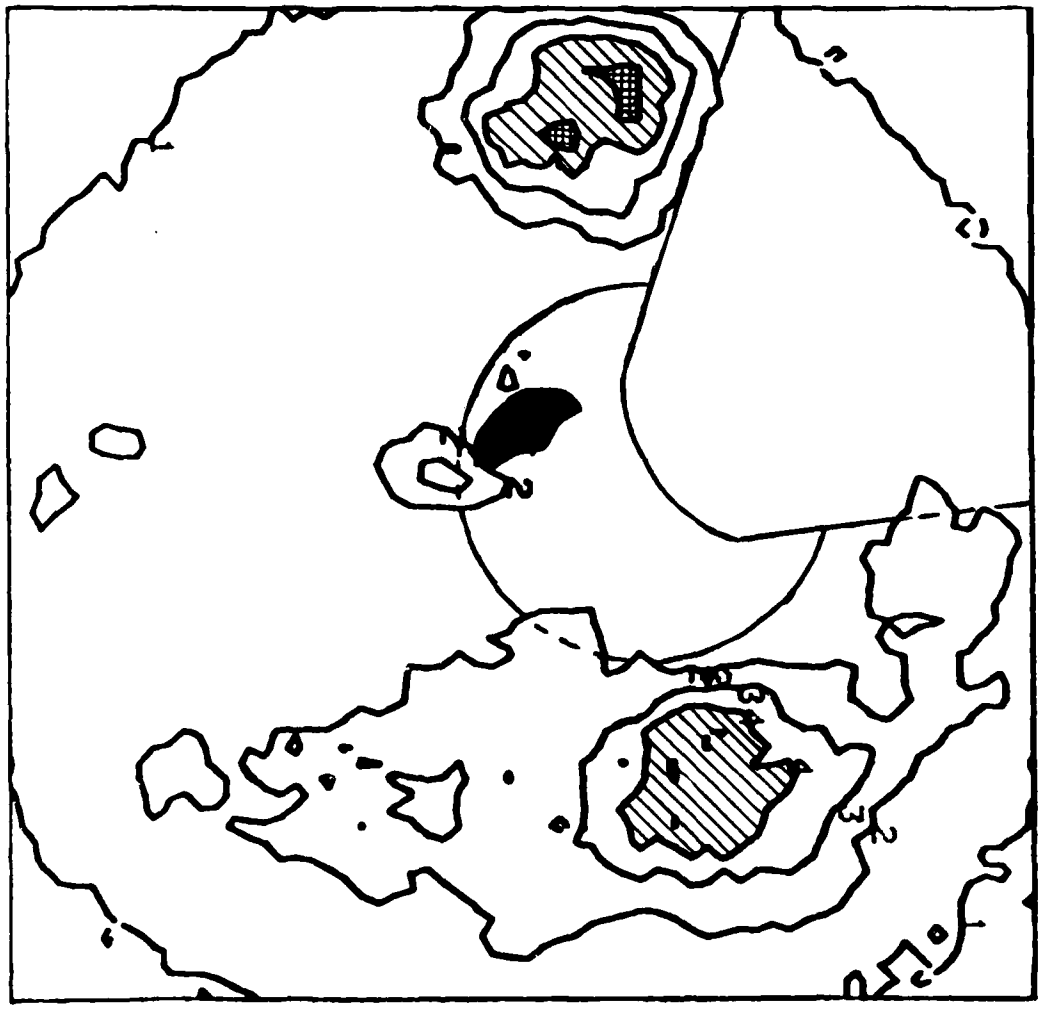

81-6-155-21

In each of the frames one can observe the flame contour pattern from the fuel nozzle above and just to the left of the center tube and the flame pattern from the nozzle just below the fiberscope. The time between each frame is 200 μsec, and the exposure time per frame is 100 μsec. The motion of the flame from the upper nozzle can be followed from frame-to-frame as it pinches into two pieces and moves downward slightly. By frame 6 (Fig. 5.7) the upper flame has completed its division, and the severed piece travels down the combustor, becoming smaller in apparent size and cooling. The lower flame, meanwhile spreads sideways in both directions and cools in the last several frames. The lower flame consists of two distinct hot zones in frame one. By frame 5 the lower flame has contracted slightly and shifted to the right. The left hand hot zone in frame 5 has cooled and breaks up into three pieces. By frame 8 the hot zones have further broken up and the flame has stretched further to the right in front of the center tube. In figure 9 the lower flame begins streaching to the left and a single hot zone becomes centered in the pattern. The detailed motion of the lower flame in particular appears somewhat irregular. The camera framing rate is not quite fast enough to follow all the flame developments. The overall flame motion around and down the combustor liner can be observed quite easily, however, in the motion pictures.

6. CONCLUSIONS AND RECOMMENDATIONS

During this program we demonstrated the feasibility of viewing flame patterns and their motions with a small fiber optic probe in a high pressure gas turbine combustor. The flame motion was recorded and reduced in speed over 200 times with high speed motion cameras. Laser illumination of the fuel spray from fibers included in the same probe was also demonstrated. In addition, measurements of flame spectra at visible wavelengths was examined and a mean color temperature was inferred. Another diagnostic method was examined that measured the flame motion frequency. A possible coupling to an acoustic resonance was observed.

The placement of the probe to view downstream from behind the fuel nozzles may not have been the best choice for location. Especially when measuring flame spectra, the view through the burning fuel spray and recirculating soot caused a sizeable wavelength dependent transmission function and filtered the blue part of the spectrum. With proper water cooling a probe could be placed in the side of the burner liner, or for special cases look through a dilution hole in the side of the liner. An in/out actuator could also be used to allow intermittent viewing through the side of the liner. The actuator could also act as a safety device to withdraw the probe in case of overheating. For certain measurements such as the high speed motion pictures and flame spectra, which can be taken in a period of a couple seconds, the probe need not remain in the burner hot region for a long period of time and intermittent viewing would be adequate.

The probe built under the current program was fixed in position, but had a wide viewing angle (90°) to see as much of the combustor as possible. If the probe is actuated for rotation of view then a narrow angle view could be used and the combustor scene scanned. A reduction of the field-of-view (or viewing angle) improves the resolution but decreases the range of focus. On the current probe the view remained in focus from about 2 cm to infinity. If the FOV is considerably narrower, then the range of focus can be severely restricted, and in this case an actuated focus adjust would be necessary. A more ideal and elaborate probe, then, would be one that is actuated for in/out motion, rotation of the view, and focus adjust, and have a moderate FOV so that there is a reasonable depth of field. For special applications where you might want to look at surface detail a narrow FOV with a fine focus adjust would be required.

The reflection of light from the surface of the liner is diffuse and amounts to only a few percent of the incident light. Since film has a small dynamic range, we could not clearly photograph the linear surface in the presence of the bright luminous flame. To obtain a view of the combustor surface the light incident directly from the flame would have to be filtered, blocked, or excluded from the FOV so that a greater exposure can be taken from the

surface relected light. An additional fiber optic illuminator could also be used to illuminate the surface with a laser or an incoherent source. An incoherent source with high intensity blue light from a xenon arc source that runs at a much higher color temperature than the flame would make a good illuminator, for example, in the presence of flame radiation. A blue filter could be used at the receiver to block most of the flame radiation. Laser illumination allows for a convenient small design since only a single fiber is needed to transmit the entire beam. The laser produces both modal and speckle interference patterns, however, that could make the surface reflection more difficult to interpret in certain circumstances.

In general, fiber optics allow optical data and images to be taken and transferred out of limited access areas where it is impractical or difficult to do so with conventional optical components such as relay lenses, reflectors, telescopes, etc. Moreover, the fibers themselves may act as sensing elements in special design configurations. One such example is a recently designed temperature sensor that has a short section of fiber doped with rare earth (Ref. 17). The application of fiber optic viewing devices to combustors will be as an aid to understanding their operation and failure modes, and to help in future design considerations and changes. The viewing probe can determine such things as: the location and motion of the flame or hot burning zone in relation to the combustor surfaces; observation of the mixing of burning fuel and turbulent air; recirculation of the flame; development of liner damage; accumulation of coking deposits; fuel spray patterns; flame color temperature measurements; and combustor acoustics that couple to the flame pattern. With additional probes to inject focused laser beams, laser diagnostics such as LDV and particle scattering to determine soot and fuel spray velocities and densities would be possible. Greater access would be required for injection of the laser beam at larger angles to the fiberscope view.

One of the more important uses of the fiberscope may be to measure flame color temperature. The possibility of this being done was indicated in section 5.2 and by Fig. 4.10. With the ability to take rapid electronically scanned spectra and use fast electronic calculations, the equation that describes the emission from a luminous soot flame could be fit to a mean temperature in the field-of-view of the optical receiver. If a few pixels from the fiberscope output or only a single fiber probe is used, a narrow angle view will be defined and the mean temperature will be taken along a path length extending outward in the direction of view. The measured temperature is weighted heavily to the higher temperatures of the distribution along the path. If a very hot region were in the view the temperature would correspond more closely to the higher temperatures of that region. The application of color temperature measurement with a small optical fiber probe near the turbine inlet may prove useful as a diagnostic tool to help measure temperature profiles and possibly in the future as an engine control. We recommend that this aspect of the program be given the first priority for further investigation

and a demonstration be arranged with a small atmospheric pressure oil burning flame. The demonstration experiment would make a comparison of the optical fiber probe measurement, a thermocouple measurement over the viewing path, and the sodium or soot reversal measurement technique (Kurlbaum) that has been used in the past (Ref. 4) to measure flame temperatures over a path length extending through flames. A theoretical analysis of the emissivity function should also be made to more clearly define the measured temperature in relation to the temperature distribution function and soot particle density. At the turbine inlet, where the temperatures are cooler than the flame upstream, scattered light from the flame may also give a small contribution to the soot particle emission as discussed by Atkinson and Strange in Ref. 3 with respect to reflected light when measuring surface temperatures.

If infrared transmitting fibers became available in the next year the radiation from CO_2 and H_2O vibration bands along with the soot emission could be measured over a band of wavelengths. In this case the emitting zone would be more optically dense and consequently more blackbody like. This feature makes the temperature calculation easier and possible more reliable. At the other end of the spectrum a quartz fiber could be used to transmit the uv banded spectra of OH. The use of laser induced fluorescence (LIF) as demonstrated by Chan and Daily in a methane burner (Ref. 12) could also be investigated with the use of an additional uv laser illuminating fiber. The difficulty of applying LIF to a sooting flame, however, has not been reported.

REFERENCES

1. R. M. McCord, "Fiber Optic Probes Monitor Engine Condition," Mech. Eng., January 1981, pgs. 36-40.

2. W. Drinkuth, W. G. Alwang, and R. House, "Laser Proximity Probes for the Measurement of Turbine Blade Tip Running Clearances," ISA ASI 74228 (133-140), 1974.

3. W. H. Atkinson, R. R. Strange, "Pyrometer Temperature Measurements in the Presence of Reflected Radiation," ASME Publication 76-HT-74.

4. A. G. Gayden, H. G. Wolfhand, Flames - Their Structure, Radiation and Temperature, Fourth Edition 1979, Halsted Press, a Division of John Wiley & Sons, New York.

5. N. S. Kapany, Fiber Optics, Academic Press, New York, 1967, Chapter 4.

6. V. B. Vienberg and L. S. Trofinova, "The Resolution of a Combination of Butt-Joined Fiber Components," Sov. J. Opt. Tech. 44, 260 (1977)

7. W. P. Siegmund, "Fiber Optics - Principles, Properties & Design Considerations," American Optical Fiber Optics Division, Southbridge, MA.

8. Beretta, F., Cavaliere, A., D'Alessio, A., "Visible and U.V. Spectral Emission and Extinction Measurements in Oil Spray Flame," Comb. Sci. and Tech. 22, pp. 1-15 (1980).

9. R. W. Claus, "Spectral Flame Radiance From a Tubular-Can Combustor", NASA Technical Paper 1722, February 1981.

10. L. E. Drain, The Laser Doppler Technique, John Wiley and Sons, Ltd. (1980); also "Doppler Velocimetry," Laser Focus, October 1950.

11. D. J. Holve, "In Situ Optical Particle Sizing Technique," J. Energy 4, 176 (1980).

12. C. Chan and J. W. Dailey, "Measurement of Temperature in Flames Using Laser Induced Fluorescence Spectroscopy of OH" App. Optics 19, 1963 (1980).

13. A. C. Eckbreth, "Application of Laser Raman Scattering Diagnostic Techniques to Practical Combustion Systems," Project Squid, Tech. Report, UTRC-4-DU.

REFERENCES (Cont'd)

14. J. A. Shirley, R. J. Hall, and A. C. Eckbreth, "Investigation of the Feasibility of CARS Measurements in Scramjet Combustion," NASA Contractor Report 159280, July 1980.

15. Beretta, F. et al., "Laser Light Scattering, Emission/Extinction Spectroscopy and Thermogravimetric Analysis in the Study of Soot Behavior in Oil Spray Flames," Eighteenth International Symposium on Combustion, Ontario, Canada, August 1980.

16. P. J. Foster, "Calculation of the Optical Properties of Dispersed Phases," Combust. Flame, Vol. 7, September 1963, pp. 277-282.

17. W. H. Glenn, W. W. Morey, and E. Snitzer, "Analysis and Preliminary Design of Optical Sensors for Propulstion Control," NASA Lewis Research Center Contract Report NASA CR-159468, Marcy 1979.